



Publicly Accessible Penn Dissertations


1-1-2015

An Urban-Conscious Rapid Wind Downscaling Model for Early Design Stages

Jihun Kim

University of Pennsylvania, jihun@design.upenn.edu

Follow this and additional works at: <http://repository.upenn.edu/edissertations>

 Part of the [Architecture Commons](#), and the [Environmental Sciences Commons](#)

Recommended Citation

Kim, Jihun, "An Urban-Conscious Rapid Wind Downscaling Model for Early Design Stages" (2015). *Publicly Accessible Penn Dissertations*. 1076.

<http://repository.upenn.edu/edissertations/1076>

This paper is posted at ScholarlyCommons. <http://repository.upenn.edu/edissertations/1076>

For more information, please contact libraryrepository@pobox.upenn.edu.

An Urban-Conscious Rapid Wind Downscaling Model for Early Design Stages

Abstract

Assessments of urban contexts using existing microclimate models mostly fall short, when considering topographies along with complex layouts of buildings and streets, regardless of their significant influences on building performances and outdoor environments. The challenge exists mainly due to model's inherent complexities and the associated high computational costs. This becomes especially challenging at early design stages when time, expertise, and computational resources are limited, even though the opportunities for performance enhancement are greater than at later stages.

This dissertation develops a wind downscaling model that can rapidly assess urban contexts to relate climate data in a large spatial resolution for a smaller-scale site. Surrounding slopes and terrains, up to a few kilometers in diameter, are considered to predict wind pressure on the volumetric boundary of a neighborhood and local wind speed. The new model strives for prediction accuracy and computational efficiency by employing the capacities of a computational fluid dynamics (CFD) simulation and of an existing mathematical method.

The proposed model is composed of three parts: pressure database, speed database, and interpolation. The databases store wind data for existing urban contexts that are generated with CFD simulations. Using the databases, the interpolation approximates the pressure outcomes for a new urban context; thus, real-time CFD runs can be avoided for the model users. Independent development of data for pressure and speed facilitates the flexibility and expandability of the model.

The proposed model showed an acceptable prediction accuracy, with average errors of less than 10%, compared to the full-scale CFD simulation for the same territorial scope. An exceptional computational efficiency is also shown, with a runtime in 0.308 seconds, which is 16568 times faster than the CFD simulation. This rate allows creation of a yearlong prediction in a few tens of minutes with a personal desktop computer. For non-experts, the pertinence of the model is enhanced with a limited number of parameters, making it easily adaptable during early design stages of buildings and urban design scales. Geometric sensitivities are embedded for incremental study, which is crucial to finding optimal solutions, toward more efficient, yet healthier, urban environments.

Degree Type

Dissertation

Degree Name

Doctor of Philosophy (PhD)

Graduate Group

Architecture

First Advisor

Ali M. Malkawi

Second Advisor

Yun K. Yi

Keywords

Database and interpolation, Early design stages, Neighborhood scale, Rapid wind downscaling, Topography and terrain, Urban contexts

Subject Categories

Architecture | Environmental Sciences

**AN URBAN-CONSCIOUS RAPID WIND DOWNSCALING MODEL
FOR EARLY DESIGN STAGES**

Jihun Kim

A DISSERTATION

in

Architecture

Presented to the Faculties of the University of Pennsylvania

in

Partial Fulfillment of the Requirements for the

Degree of Doctor of Philosophy

2015

Supervisor of Dissertation

Co-Supervisor of Dissertation

Ali M. Malkawi

Yun Kyu Yi

Professor of Architecture

Assistant Professor of Architecture

Graduate Group Chairperson

David Leatherbarrow, Professor of Architecture

Dissertation Committee

Jennifer Lukes, Associate Professor of Mechanical Engineering and Applied
Mechanics

ABSTRACT

AN URBAN-CONSCIOUS RAPID WIND DOWNSCALING MODEL FOR EARLY DESIGN STAGES

Jihun Kim

Ali M. Malkawi

Yun Kyu Yi

Assessments of urban contexts using existing microclimate models mostly fall short, when considering topographies along with complex layouts of buildings and streets, regardless of their significant influences on building performances and outdoor environments. The challenge exists mainly due to model's inherent complexities and the associated high computational costs. This becomes especially challenging at early design stages when time, expertise, and computational resources are limited, even though the opportunities for performance enhancement are greater than at later stages.

This dissertation develops a wind downscaling model that can rapidly assess urban contexts to relate climate data in a large spatial resolution for a smaller-scale site. Surrounding slopes and terrains, up to a few kilometers in diameter, are considered to predict wind pressure on the volumetric boundary of a neighborhood and local wind speed. The new model strives for prediction accuracy and

computational efficiency by employing the capacities of a computational fluid dynamics (CFD) simulation and of an existing mathematical method.

The proposed model is composed of three parts: pressure database, speed database, and interpolation. The databases store wind data for existing urban contexts that are generated with CFD simulations. Using the databases, the interpolation approximates the pressure outcomes for a new urban context; thus, real-time CFD runs can be avoided for the model users. Independent development of data for pressure and speed facilitates the flexibility and expandability of the model.

The proposed model showed an acceptable prediction accuracy, with average errors of less than 10%, compared to the full-scale CFD simulation for the same territorial scope. An exceptional computational efficiency is also shown, with a runtime in 0.308 seconds, which is 16568 times faster than the CFD simulation. This rate allows creation of a yearlong prediction in a few tens of minutes with a personal desktop computer. For non-experts, the pertinence of the model is enhanced with a limited number of parameters, making it easily adaptable during early design stages of buildings and urban design scales. Geometric sensitivities are embedded for incremental study, which is crucial to finding optimal solutions, toward more efficient, yet healthier, urban environments.

TABLE OF CONTENTS

ABSTRACT.....	II
LIST OF TABLES	VII
LIST OF FIGURES.....	VIII
CHAPTER 1 INTRODUCTION.....	1
1.1 BACKGROUNDS.....	1
1.2 LITERATURE REVIEW	3
1.2.1 Climate Data for Building Studies.....	3
1.2.2 Climate Downscaling	4
1.2.3 Issues in Wind Downscaling.....	5
1.2.4 Existing Methods for Wind Downscaling	9
1.3 OBJECTIVES.....	13
1.4 DISSERTATION OUTLINE.....	15
CHAPTER 2 METHODOLOGICAL FRAMEWORK	16
2.1 OVERALL SYSTEM STRUCTURE	16
2.2 MODEL CONSIDERATIONS.....	19
2.2.1 Urban Scales	20
2.2.2 Wind Data Types	22
2.2.3 Terrain Model.....	23
2.3 ACCEPTABLE RANGE OF ERRORS	25
2.4 TARGET COMPUTATIONAL EFFICIENCY	27
CHAPTER 3 DATABASES AND INTERPOLATION SYSTEM	28
3.1 PRESSURE DATABASE.....	28
3.1.1 Parameterization.....	29
3.1.2 Geometric Sampling	30

3.1.3 CFD Simulation.....	31
3.1.4 Pressure Database	32
3.2 SPEED DATABASE	34
3.2.1 Geometric Sampling	34
3.2.2 CFD Simulation.....	35
3.2.3 Reduction Ratio	35
3.3 INTERPOLATION	36
3.3.1 Pressure Approximation	37
3.3.2 Refinement with Speed	38
CHAPTER 4 PRESSURE DATABASE DEVELOPMENT	41
4.1 INITIAL DATABASE WITH 11 SAMPLES.....	41
4.1.1 Parameterization of Site Geometry	42
4.1.2 Range of Parameters	43
4.1.3 Sampling with Varying Parameters	46
4.1.4 Wind Pressure Assessment for Samples.....	47
4.2 INITIAL INTERPOLATION TEST	49
4.3 ACCURACY IMPROVEMENT	53
4.3.1 Increase the Number of Samples.....	54
4.3.2 Accuracy Test for Neighborhood Volume	58
4.3.3 Sensitivity Test for Topographic Conditions.....	62
4.4 SUMMARY	66
CHAPTER 5 SPEED DATABASE DEVELOPMENT.....	67
5.1 GEOMETRIC CONDITIONS	67
5.1.1 Terrain.....	67
5.1.2 Slope.....	69
5.2 WIND SPEED ASSESSMENT	70
5.3 WIND REDUCTION RATIOS.....	73
5.4 SUMMARY	75
CHAPTER 6 MODEL EVALUATION	76

6.1 TEST CONDITION	77
6.2 RESULT ANALYSIS	78
6.2.1 Comparison with No-Terrain.....	78
6.2.2 Comparison with Terrain	81
6.2.3 Computational Efficiency	85
6.3 SUMMARY	86
CHAPTER 7 CONCLUSION	87
7.1 RESEARCH OVERVIEW.....	87
7.2 FINDINGS AND IMPLICATIONS	89
7.2.1 Prediction Goals	89
7.2.2 Modeling Objectives	90
7.3 LIMITATIONS AND FUTURE PERSPECTIVE	91
7.3.1 Geometric Simplification.....	91
7.3.2 Defined Ranges of Parameters	92
7.3.3 Fixed Number of Pressure OuputS	93
7.3.4 Leeward Wind Translation.....	94
7.3.5 Validation	95
7.4 CONCLUDING REMARK	96
BIBLIOGRAPHY	97
INDEX	104

LIST OF TABLES

Table 1 Urban climate scales with territorial limits for Philadelphia, PA.....	21
Table 2 Atmospheric boundary layer parameters (ASHRAE 2001)	24
Table 3 Computer specifications in use	27
Table 4 Range of parameters for neighborhood size and topography	45
Table 5 Varying parameters for sample site geometries in the database	47
Table 6 Wind pressure data for the sample site geometries (Pascal).....	48
Table 7 Parameters of the urban condition for prediction test.....	49
Table 8 Normalized errors in initial model prediction (%)	53
Table 9 Computational time with number of samples (hours)	54
Table 10 Average error with more samples on west surface (%).....	55
Table 11 Average error with more samples on south surface (%)	57
Table 12 Normalized errors for west surface with different neighborhood lengths (%).....	60
Table 13 Normalized errors on west surface with different neighborhood heights (%).....	61
Table 14 Parameters for four site geometries.....	63
Table 15 Wind patterns by terrains on slopes – city center and urban.....	71
Table 16 Wind patterns by terrains on slopes – industrial and unobstructed.....	72
Table 17 Parameters for the test condition	77
Table 18 Prediction errors for the no-terrain condition (%).....	80
Table 19 Prediction errors for the terrain-integrated solution (%).....	84
Table 20 Computational time for comprehensive model prediction (seconds).....	85

LIST OF FIGURES

Figure 1 Climate and urban context in building performance assessment.....	1
Figure 2 Significance of rapid urban climate model.....	3
Figure 3 Leeward wind flow issue in urban wind downscaling	6
Figure 4 Topographic effect on urban wind downscaling	7
Figure 5 Homogeneity in surrounding terrain for a local site	8
Figure 6 Overarching system structure.....	17
Figure 7 Pressure measurement point, numbers for locations on neighborhood surfaces....	23
Figure 8 Pressure database with surrounding slopes and neighborhood volume.....	28
Figure 9 Speed database with terrain and slope	34
Figure 10 Interpolation system with pressure and speed database	36
Figure 11 Parameterization of site geometry with slope and neighborhood volume.....	42
Figure 12 Range of regional wind speeds in U.S. cities (m/s).....	46
Figure 13 Sample site geometries for CFD simulations.....	47
Figure 14 Site geometry with mixed-slope for initial prediction testing.....	50
Figure 15 Initial test result with small number of samples for pressure database (Pascal) ...	51
Figure 16 Initial test result at each point of the surfaces (Pascal).....	52
Figure 17 Accuracy increase with more samples on west surface (Pascal).....	55
Figure 18 Accuracy increase by more samples on south surface (Pascal).....	57
Figure 19 Predicted pressure on west surface with different neighborhood lengths (Pascal)	59
Figure 20 Predicted pressure on west surface with different neighborhood heights (Pascal)	61
Figure 21 Four site geometries for prediction test	62
Figure 22 Predicted pressure on west surface for four site geometries (Pascal).....	63
Figure 23 Predicted pressure on east surface for four site geometries (Pascal)	64

Figure 24 Predicted pressure on south surface for different site geometries (Pascal)	65
Figure 25 Geometrical input of each terrain type for CFD simulations.....	68
Figure 26 Slope, added to the terrain geometry for CFD simulations	69
Figure 27 Wind reduction ratio for sloped terrain, normalized by flat terrain.....	74
Figure 28 Model test with the CFD simulation	76
Figure 29 Urban terrain on the test condition.....	77
Figure 30 Pressure outcome, compared with no-terrain solution (Pascal).....	79
Figure 31 Pressure outcome, compared with the terrain-integrated solution (Pascal)	82
Figure 32 Pressure outcome at each point of the surfaces (Pascal).....	83

CHAPTER 1 INTRODUCTION

1.1 BACKGROUNDS

Urban areas have unique climatic behaviors in comparison to rural areas, mainly due to buildings, roads, and anthropogenic heats that together modify the heat balance of a regional climate (Santamouris 2001, Oke and Maxwell 1975, Park 1986, Johnson et al. 1991, Arnfield 2003, Oleson et al. 2008). The urban heat islands, one of the main characteristics of urban climate, cause outdoor thermal discomfort (Rizwan, Dennis, and Chunho 2008), while generating detrimental smog with pollutant emission (Jebson 2007). At the same time, buildings in an urban area may consume approximately 1.8 times more energy for cooling demands than those in a rural area (Saneinejad et al. 2012, Allegrini, Dorer, and Carmeliet 2012). Therefore, accurate assessment of urban contexts is a critical factor for creating high-performance buildings and healthier urban conditions.

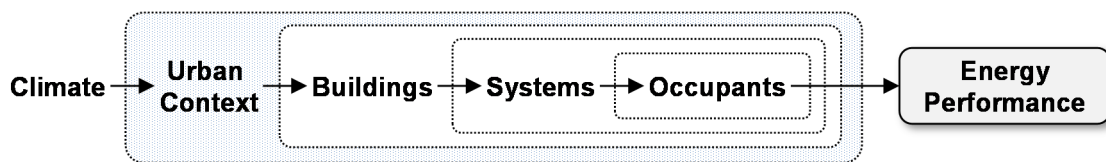


Figure 1 Climate and urban context in building performance assessment

Despite their significances, assessments of urban context, however, are often over-simplified or outright ignored, Figure 1, while much emphasis is placed on buildings, systems efficiency, and occupants' behavior as the main players in

building energy simulation (Ratti, Baker, and Steemers 2005, Baker and Steemers 2003). This is because model developments and simulation capacities are still in their infancy. With their inherent complexities and high computational costs, existing models fall short of considering large topographies and complex layout of buildings and streets (Mirzaei and Haghghat 2010, Martilli 2007). At the same time, the lack of models in a proper scale was identified as a problem for urban designers (Larsen 2011). This issue has been receiving growing attention for its crucial impact on global climate changes (WHO 2008).

Due to its chaotic nature, wind is particularly hard to predict within urban contexts, yet it is important for the heat balance of a microclimate. Wind influences convection and advection of urban heat balance, which in turn affects the heat balance of a climate condition as whole, together with radiation and conduction (Haeger-Eugensson and Holmer 1999, Incropera 2011, Zhao, Hobbs, and Ord 2008). It stands to reason that wind has been identified as a main climate factor to disperse excessive heat and smog from urban areas, minimizing the heat island effects (Jebson 2007).

Because of these emergent needs and their significances, developing a wind prediction model that assesses the urban context has become the overarching goal of this dissertation, Figure 2. By accounting for topographies and buildings, wind data that represents a region up to a few kilometers is downscaled for a smaller neighborhood scale. As the input, a whole year's climate data is considered for the model's comprehensiveness for use in building-scale studies.

The proposed model aims to reduce uncertainties in urban wind predictions, which may support further research on energy efficiencies, outdoor wind comfort, and urban heat islands.

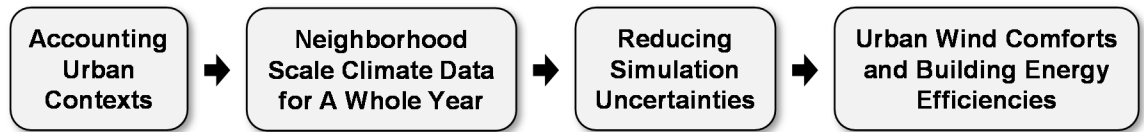


Figure 2 Significance of rapid urban climate model

1.2 LITERATURE REVIEW

To guide the development of a new model, the literature review is conducted, beginning with defining the climate data for the urban scale of interest. For better representation of local conditions, an existing technique “climate downscaling” is introduced; its key issues are identified and provided with potential solutions by existing methods.

1.2.1 CLIMATE DATA FOR BUILDING STUDIES

In building simulation and urban climatology communities, various territorial scales of climate are defined for analysis conveniences, even though weather – the base data of climate definitions – is a continuous phenomenon (Baklanov and Nuterman 2009, Hewitson and Crane 1996, Oke 1987). Various scales also serve to study different problem domains, such as wind environment within a building complex,

thermal effects of wind on the human body, contaminant dispersion around a building, thermal comfort in outdoor spaces, and the effects of human activities on regional climate. A domain of heat and air flow studies for a human is as small as around 1m in diameter, while urban scale domains range from 10km~100km in diameter (Murakami et al. 1999).

For building-scale studies, climate datasets at the regional scale are generally used, which are produced by the National Renewable Energy Laboratory. This climate data is called “Typical Meteorological Year” (TMY), a collection of 8760 hours of weather data for a fixed location (Marion and Urban 1995). Wind speed and direction data is included along with temperature, humidity, solar radiation, and precipitation. A TMY is synthesized from 30 years of weather data to represent long-term statistical trends and patterns. The current (third) version, TMY3, uses a recent weather database up to year 2005, for 1020 locations in the United States (Wilcox and Marion 2008). For the general life spans of buildings, this long-term representation has an advantage over real-time data from a personal weather station that may only reflect short-term climate behavior (Crawley 1998).

1.2.2 CLIMATE DOWNSCALING

Even though TMY represents the climatic characteristics of a region, it hardly represents the local climate that is modified by buildings, streets, trees, anthropogenic activities, and other heterogeneous characteristics of an urban context. This is mainly because weather data for TMY is generally recorded at a

long distance, typically at an airport or open field, far away from city centers where most urban constructions occur (Wilcox and Marion 2008). To overcome this discrepancy, “downscaling,” the term in climatology, (often called “localization”) is used to relate climate data in a large spatial resolution for a smaller scale site that is useful for different types of studies (Hewitson and Crane 1996, Murphy 1999). Downscaling, therefore, is regarded as the first step in building studies towards understanding the impact of surrounding conditions (Clarke 2001).

1.2.3 ISSUES IN WIND DOWNSCALING

Even though wind downscaling may produce more relevant data for small scale studies, inherent issues exist, mainly due to the climate dataset being recorded at a fixed distance location. The current section identifies three issues: leeward wind flow, lack of topographic effect, and homogeneity in surrounding terrain.

1.2.3.1 LEEWARD WIND FLOW

To illustrate the first issue “leeward flow,” downscaling of regional wind data for a local site in two opposite directions is shown in Figure 3. If wind progresses from a weather record location to a specific local site, a wind downscaling may properly account for the urban condition, which is geographically situated in the direction of the wind. This is called a windward condition (Figure 3a). However, the same logic does not hold in a leeward condition (Figure 3b) if wind progresses away from the site. This issue causes problems in using TMY data as boundary conditions, since

the regional climate data from the opposite location is unavailable in most situations.

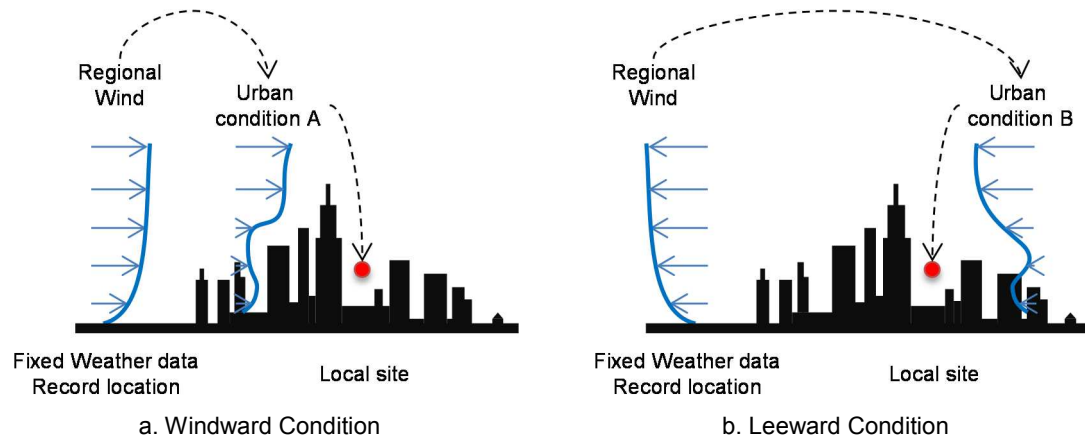


Figure 3 Leeward wind flow issue in urban wind downscaling

Generating a new dataset for another location is one of the existing approaches with available climate data. This includes “stochastic weather generation” (Bouhaddou et al. 1997, Degelman 2003) and “spatial regression” with a few variables, such as site elevation (Semenov and Brooks 1999). Even if a general pattern can be found similar to the analyzed base weather files, these models do not account for geometries and materials of urban conditions that significantly affect wind flow and related urban heat balances (Sun et al. 2011). This oversight is primarily because the model was originally targeted for agricultural uses, neglecting the unforeseen urban obstacles.

1.2.3.2 LACK OF TOPOGRAPHIC EFFECT

Lack of topographic effect is the second issue in wind downscaling. In general, topography, which becomes more prominent in mountainous sites, plays an

important role in urban climate by influencing airflow and heat prediction, often more than building and street geometries (Troude et al. 2002, Wanner H. 1989). Yet, this is barely addressed in existing climate downscaling models, where a flat terrain is assumed for simplification in building simulations. Figure 4 illustrates how an existing downscaling model works with flat topography (a), whereas it is hard to address the effect of topography on a sloped condition with the same urban contexts (b).

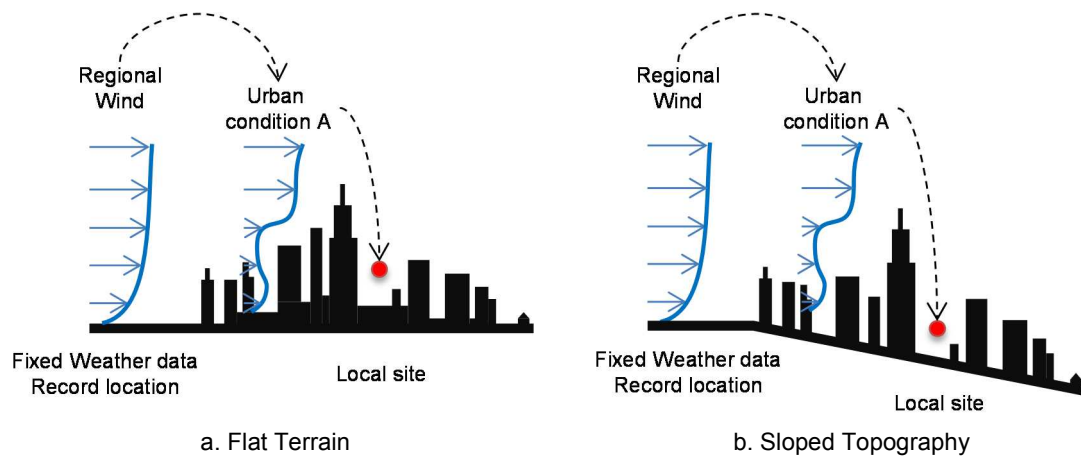


Figure 4 Topographic effect on urban wind downscaling

One recent development proposes the use of a “Macro” scale model that was originally developed for national weather forecasts, considering topographic conditions of the entire surface of earth in a very low spatial resolution (Hensen and Lamberts 2011, Malkin 2009). The main benefit is that downscaled climate data is available within 14 km of any given location in the United States, with more than 55,000 virtual observed locations. This may better represent a local site than the current TMY development with 1020 locations (Section 1.2.1). However, resultant climate data from a macro -scale model still needs downscaling to reflect

actual urban conditions whose microclimates are dominated by individual buildings and streets in the neighborhoods as well as by the topographic conditions.

1.2.3.3 HOMOGENEITY IN SURROUNDING TERRAIN

The third issue arises due to the overly simplified use of terrain effect on wind downscaling. Building simulation and wind engineering communities generally assume homogeneity in terrain conditions around a site with a simple built environment (ASHRAE 2001, ASCE 2003), as illustrated in an aerial view at Figure 5a. With empirically driven wind reduction factors for terrain types, vertical wind speed profiles are generated for any direction of wind. This model was originally formulated for the urban scale designs to account for urban boundary thickness (Oke 1987).

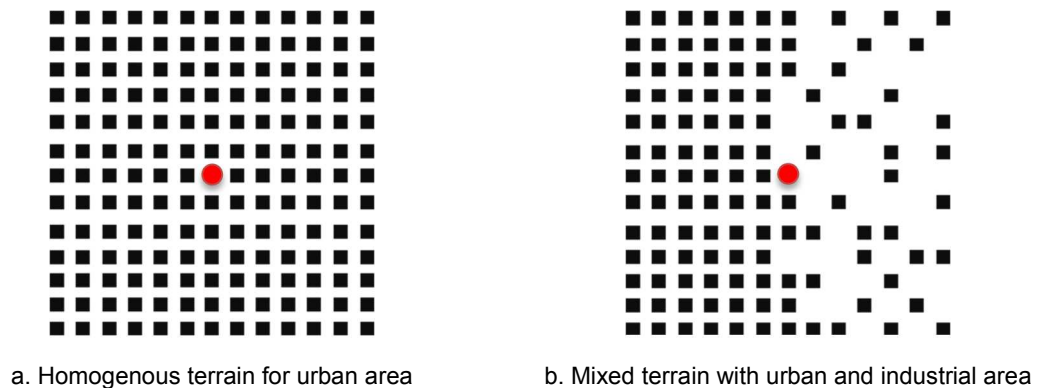


Figure 5 Homogeneity in surrounding terrain for a local site

However, the diversity in urban contexts would better reflect realistic urban conditions for the building and neighborhood scale as illustrated in Figure 5b. One type of urban contexts, such as dense city center at the west of the site, affects wind downscaling for the particular wind direction. However, downscaling with

another type of urban context, such as industrial area at the east of the site, may result in a significant difference for the opposite wind direction.

Even if detailed wind-tunnel tests may provide solutions, it is unrealistic to apply their results to diverse terrain conditions. Such tests entail prohibitive resources and require expertise, especially for large-scale sites in early design stages. Moreover, the limited availability of regional wind data prohibits accounting for various terrains, which also caused the first issue, “leeward flow.”

1.2.4 EXISTING METHODS FOR WIND DOWNSCALING

In search of potential solutions to the identified issues (Section 1.2.3), existing methods are reviewed, including canyon model, nodal network method, and Computational Fluid Dynamics. Their capacities and limitations inform the objectives of a new model development.

1.2.4.1 CANYON

Canyon model is the first existing downscaling method, which has been developed for the past forty years, analyzing large-scale areas for urban heat island effects, their impact on human health, and their energy saving potentials. Of particular interest here is Oke (1971) who maintains that a climate within an urban area behaves distinctly from an upper atmosphere layer, creating an urban boundary layer, which is different from a suburban area (Oke and Maxwell 1975, Oke and East 1971, Oke 1976). This hypothesis, called “Canyon,” has been developed and

validated for urban-scale studies (Masson 2006, Masson 2000). The Canyon model has been further developed and its impact on building performance in a city has been researched (Sun et al. 2011).

Meanwhile, the vertical interactions between the two vertically distinctive layers remain the main concern; wind turbulence fluxes are assumed constant for the simplification. This simplified wind accounting, called Monin-Obukhov Similarity Theory (MOS), has been identified as the main source of uncertainties (Monin and Obukhov 1954). The discrepancies in temperature prediction were observed by a site survey for wind vector and temperature 35~76 m above ground at more than 2000 undisturbed locations in Basel, Switzerland. The upper thermal condition is governed by turbulent flux different from lower level ones, showing significant deviation from MOS. Feigenwinter attributed this discrepancy to the thermal inhomogeneity from different source areas (Feigenwinter, Vogt, and Parlow 1999).

1.2.4.2 OUTDOOR NODAL MODEL

The second model, “outdoor nodal model.” was developed based on the existing indoor nodal models (or nodal network model). Indoor nodal models were developed to find the pressures of rooms, represented by a node assumed to be filled with well-mixed air (Walton 1989, Feustel and Rayner-Hoosen 1990). A floor, a ceiling, and walls constitute a node unit with pressure/height that is connected to another node by one or several links that represent airflow rates through a window, HVAC distribution systems, and other types of infiltration. This simple flow model has been incorporated in advanced thermal simulation models such as

“EnergyPlus Airflow Network Model” and “ESP-r” (Gu 2007, DOE 2005, Clarke 2001, Strachan, Kokogiannakis, and Macdonald 2008).

Outdoor nodal models, on the other hand, have recently received attention as a new type of urban climate model, taking advantage of computational lightness and acceptable accuracies for first-cut assessments in early stages of design (Yao, Luo, and Li 2011). Unlike the indoor nodal models, exterior surfaces of buildings and roads in a street canyon constitute a node that is connected to another node by links that represent interface(s) among volumetric street limits. Outdoor wind flows are assessed by utilizing the empirical data developed for large windows in indoor nodal models, assuming that airflow on outdoor streets behaves in similar ways. With thermal and airflow coupling, the outdoor nodal model has shown high potential in early stage design studies, especially for large urban areas.

However, if outdoor nodal models are used for wind downscaling, they can hardly address the topographic effects. This is because the interaction of airflow and a surface is not taken into account. This limitation comes from the fact that outdoor nodal models are based on indoor nodal models, which are developed for flow prediction among rooms, not within a single room.

1.2.4.3 COMPUTATIONAL FLUID DYNAMICS

Computational fluid dynamics (CFD) is the third existing downscaling method that numerically calculates fluid flow, mass transfer, heat transfer, and chemical reactions by solving the governing mathematical equations with a finite set of

control volumes. Its main application areas includes aerospace, automotive, civil engineering, and semiconductor industries where CFD data can complement the wind tunnel experiments or theoretical data as an engineering method (Versteeg and Malalasekera 2007).

For the past decades, CFD has been increasingly adopted in built environment analyses, such as wind assessments, studies of thermal and dynamic effects of airflow on the human body, contaminant dispersions in a building, indoor thermal comfort, and the effects of human activities on regional climate (Murakami et al. 1999, Takahashi et al. 2004, Shuzo 1997, Clarke 2001). As a more aggressive application, CFD has been used in design syntheses to enhance pedestrian wind comfort (Kim, Yi, and Malkawi 2011), thermal and ventilation performances for building envelopes (Powell 2006, Kolarevic 2003). With increased prediction accuracies (Johnson and Hunter 1998), CFD has recently become an option to replace physical wind tunnel tests in the Netherlands, for simulating a pedestrian wind environment (Willemsen and Wisse 2007, NEN 2006).

However, the high computational cost of CFD is the major drawback for whole year predictions (Zhai 2006, Blocken et al. 2011), which are crucial for studying thermal performances of buildings. More computational costs can be added to assess a large urban area. One potential solution is limiting the territorial scope within a few tens of meters while using simplified boundary conditions; this solution, however, was identified as a source of uncertainties (Mirzaei and Haghighat 2010). Another limitation is the difficulty of reproducing the urban boundary layer behaviors. This

means that the urban heat island, and its influence on the urban boundary layer and on upper atmospheric layer, will be hardly assessed (Stathopoulos 2002). Lastly, potential divergences and complexities in CFD require expert knowledge (Clarke 2001), which creates another limitation of its full use in early design stages when domain experts are not usually engaged.

Regardless of its drawbacks, CFD is the best option to consider in addressing the issues in wind downscaling for buildings and neighborhoods, compared to other reviewed methods. This is mainly because of its capacity to correlate topographies to wind prediction along with a building's geometries and materials. CFD's geometrical sensitivity allows assessing gradual changes in a slope and building typologies. Another advantage is CFD's ability to generate comprehensive information, unlike experiments, which allow investigating any locations within a domain region (Abbott and Basco 1989).

1.3 OBJECTIVES

As the main part of the dissertation, a methodological model is proposed to downscale regional wind data to represent neighborhoods in urban areas. The identified capacities of CFD are integrated, while providing potential solutions to the identified issues in downscaling. The main challenge is to reduce CFD's computational costs, while generating an acceptable range of errors. Topographies and buildings in an urban environment are the input parameters that produce outcomes that are useful for architects and urban designers in the early

design stages, when the opportunities for performance enhancement are greater than at later stages.

In addition to the CFD's own high computational demand, the new model provides a solution to save computational burdens arising from comprehensive assessment of buildings. Since whole-year assessments are important for building studies, a TMY data set is used as the regional climate data, which contains a large number of data points (8760) to be processed. For various design assessments, the total prediction run-time is desirably limited to just a few hours with a personal computer.

Considering the user group, non-CFD experts, the model aims to facilitate its pertinences in the early design stages. As an example, only a limited number of input parameters are provided to users who can analyze a complex urban system. These input parameters are geometrically sensitive; hence, the ability to conduct incremental studies will greatly benefit design professionals.

The type of output includes both wind pressure and speed, so that they can be further used for smaller-scale airflow analyses within the physical boundary of a neighborhood. Wind pressure is measured on the volumetric boundary of a neighborhood, in areas up to a few hundred meters in diameter. The resolution of pressure output is desirably high enough that its hierarchies of intensities can be assessed within a surface. Therefore, the resultant output, when used for smaller-scale studies, would better respond to the identified boundary condition problem, which cannot be solved with existing downscaling methods.

1.4 DISSERTATION OUTLINE

Chapter 2 focuses on the methodological framework of the model. It explains how the model was formulated, while the roles of the key techniques are highlighted. The modeling considerations are laid out, especially for the urban scales of interest. To measure the success of the model, the acceptable range of errors and the targeted computational efficiency are defined.

Chapter 3 elaborates the methods used to create the databases for pressure and speed, and shows how they are used in the interpolation method for analyzing a new urban context. The employed techniques are explained in detail, with focus on how they are incorporated in the workflow.

Chapter 4 and Chapter 5 develop the databases of pressure and speed, respectively. The geometric configurations are defined for the urban scale of interest. Chapter 6 evaluates the proposed interpolation method, with reference to predefined goals for prediction accuracy and computation efficiency.

Chapter 7 summarizes the findings of the study, and the initial objectives are revisited to highlight the contributions. Robustness and limitations of the model are explained, which open up potential research in the future.

CHAPTER 2 METHODOLOGICAL FRAMEWORK

The current chapter focuses on the methodological framework of the proposed wind downscaling model. It begins with how the model is formulated in three parts for surface wind pressure, local wind speed, and interpolation for a new urban context. With the predefined model's objectives (Section 1.3), the overall system structure is highlighted, even though the employed techniques are articulated and implemented in the following chapter. The model's considerations are defined, while goals are established with the acceptable range of errors and computational efficiency.

2.1 OVERALL SYSTEM STRUCTURE

The proposed methodology is formulated in three parts: pressure database, speed database, and interpolation for a new urban context, Figure 6. This approach emulates how a building-scale model, such as EnergyPlus, can predict a yearlong airflow among rooms with flexibility. Wind pressure on building surfaces is provided separately from wind speed so that they can be independently developed (DOE 2005, 2010). The method allows using an external simulation model if necessary, such as CFD for detailed airflow. To enhance computational efficiency, surface pressure data for a building come from either pre-calculated or observed data so that the user's run-time can be minimized (Stathopoulos 1984, Davenport and Hui 1982).

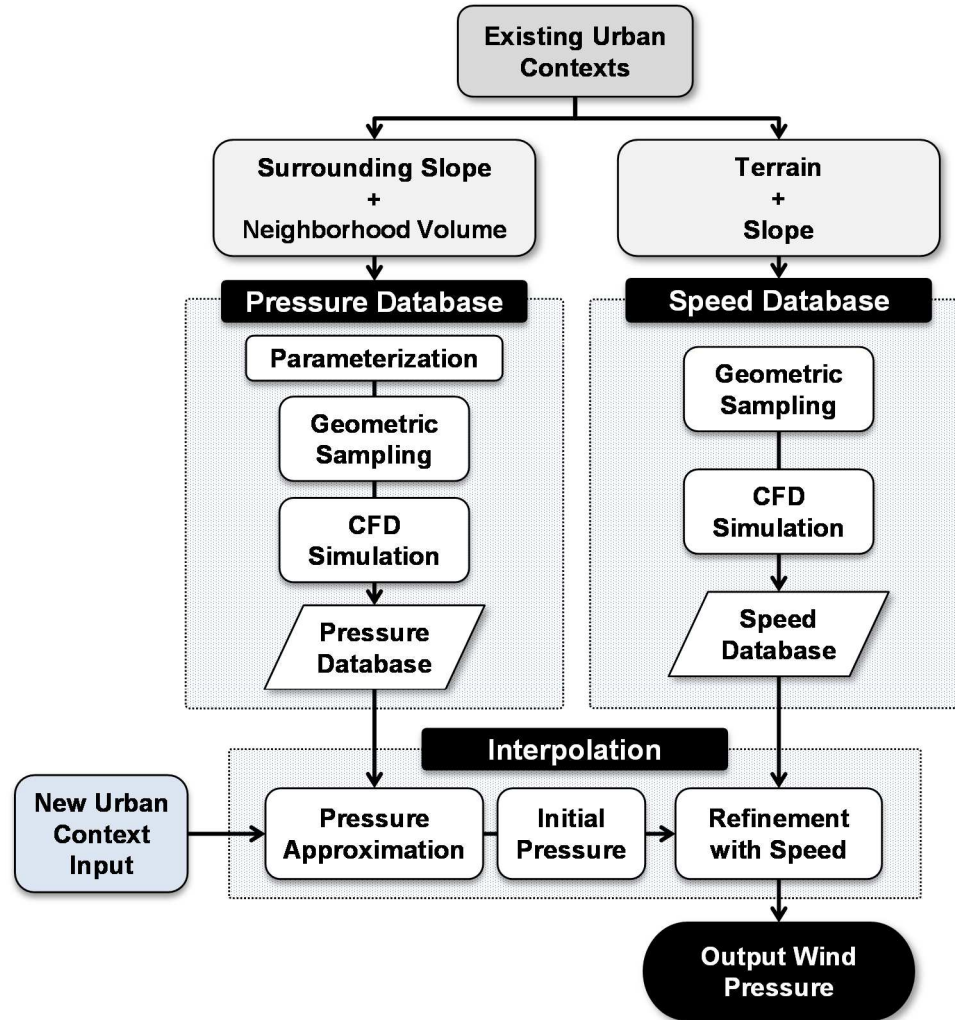


Figure 6 Overarching system structure

The first part – pressure database – generates and stores surface wind pressure on neighborhood boundaries by taking account of existing urban contexts. Surrounding slopes and neighborhood volume are the main geometric variables. Data portability is promoted by finding a minimum number of samples to represent the entire population in the database. A smaller number of samples also mean a less complicated problem to solve in approximation.

To facilitate the sampling and approximation process, the model proposes a parameterization scheme that generates urban site geometries with a limited number of variables. The main variables in the parameterization are surrounding slopes, a combination of which represents various urban conditions.

Pressure information in the database is generated by CFD simulation, whose capacities for accounting topographic effects and turbulences can be embedded in the proposed model. Site geometries are assessed to understand wind pressure impact on neighborhoods for the database. Main role of pre-processing and storing CFD simulation results in the database is to save computation time for the user to interpolate them.

The second part – speed database – generates and store local wind speed data by assessing terrain and slope in sample urban contexts, through a series of virtual wind tunnel tests with CFD simulations. Buildings and streets in terrains, the main obstruction to urban wind flow, are constructed, based on the terrain definitions in the existing mathematical method (Section 2.2.3).

Three factors constitute the speed database: 1-steepness in various slopes, 2-urban terrain types, and 3-their associated new wind reduction factor. This data-driven computation technique is similar to the pressure database, in that real-time assessment of urban contexts is avoided.

The third part – interpolation – predicts output wind pressure for new urban contexts with the pressure and speed databases. Existing approximation

techniques are employed for fast yet reasonable accuracy in engineering problem solving. The geometric parameters in the databases are analyzed and their associated pressure data are interpolated for input geometries. The initial pressure from this process counts the surrounding slopes and the volume of a neighborhood as the variables of the pressure database.

The initial pressure is refined with local wind speed that is generated by using the speed database. To integrate wind speed to surface pressure, an existing relationship of wind speed and pressure is adopted, in that an increase in a wind speed induces a corresponding increase in surface pressure to keep their constant relationship. The resultant pressure is the primary outcome of the proposed topography-conscious rapid climate downscaling model.

The proposed method, together with the databases and the interpolation, saves significant computation time that otherwise could be spent for real-time CFD-simulations of numerous buildings and large-size topographies up to few kilometers. Furthermore, the newly downscaled wind speed takes account of topographic effects that can be further utilized for building-scale airflow simulation.

2.2 MODEL CONSIDERATIONS

The current section clarifies the urban scales of interest, which helps to define the input and output for the model, regarding the wind data types. The adopted terrain




model is introduced for its important role in the interpolation process and in developing the speed database.

2.2.1 URBAN SCALES

The TMY, adopted from building studies (Section 1.2.1), represents a regional scale, up to approximately 1~5 km in diameter of an urban/suburban area, Table 1. A regional area includes smaller neighborhoods that measure 100~500 m in diameter. A neighborhood area includes multiple urban blocks, which is suitable for urban design studies with collective buildings and streets. A local area, the smallest, comprises a few buildings up to an urban block, measuring 50~100 m in diameter; two to five of these blocks compose a neighborhood. The aerial images depict Philadelphia, PA in Table 1 with dotted circles indicating how the smaller scale areas spatially fit within a larger scale domain.

The output wind data is on the neighborhood scale, which is the result of assessing urban context on a region. The scale of the model's output responds to the identified needs for urban design at Section 1.1, which is hardly addressed by the existing downscaling model for building simulation. The output data can be further utilized for the smaller local-scale studies. Even if this extra step is not part of the scope of work, it guides the data resolution of the pressure output at Section 2.3.3.

Table 1 Urban climate scales with territorial limits for Philadelphia, PA¹

<i>Climate scale</i>	<i>Philadelphia center city example</i>	<i>Approximate limits</i>	<i>Building studies</i>
<i>Local</i>		50~100 m	Few buildings / an urban block
<i>Neighborhood</i>		100 ~ 500 m	Multiple urban blocks
<i>Regional</i>		1000+ m	Urban and suburban areas

¹ Yahoo Maps

2.2.2 WIND DATA TYPES

The input wind data is provided from a TMY dataset showing regional speed and its direction. The output data type, on the other hand, includes wind pressure on the volumetric boundary of a neighborhood as well as a local wind speed for the same regional wind direction. Wind pressure is required for further uses in smaller-scale studies, such as outdoor airflow among local streets, in the same way that surface pressure on buildings is required for studies of indoor airflow among rooms (Section 2.1).

The primary output, surface wind pressure, provides for its further use in smaller scale studies by providing multiple data points for pressure hierarchies in a domain, Figure 7. For simplification, a neighborhood volume is assumed as a box with five surfaces. Four wall surfaces represent the horizontal limits on each orientation, while the top surface represents the vertical limit in the atmosphere.

On each individual surface, nine (3x3) points are predicted, which is the minimum number to differentiate the middle area from the perimeter, vertically and horizontally. Hence, pressure variations within a surface and among other surfaces further help other existing methods to predict airflow among streets within a neighborhood. This also responds to the boundary condition problem that is in low resolution as identified in Section 1.2.4.3.

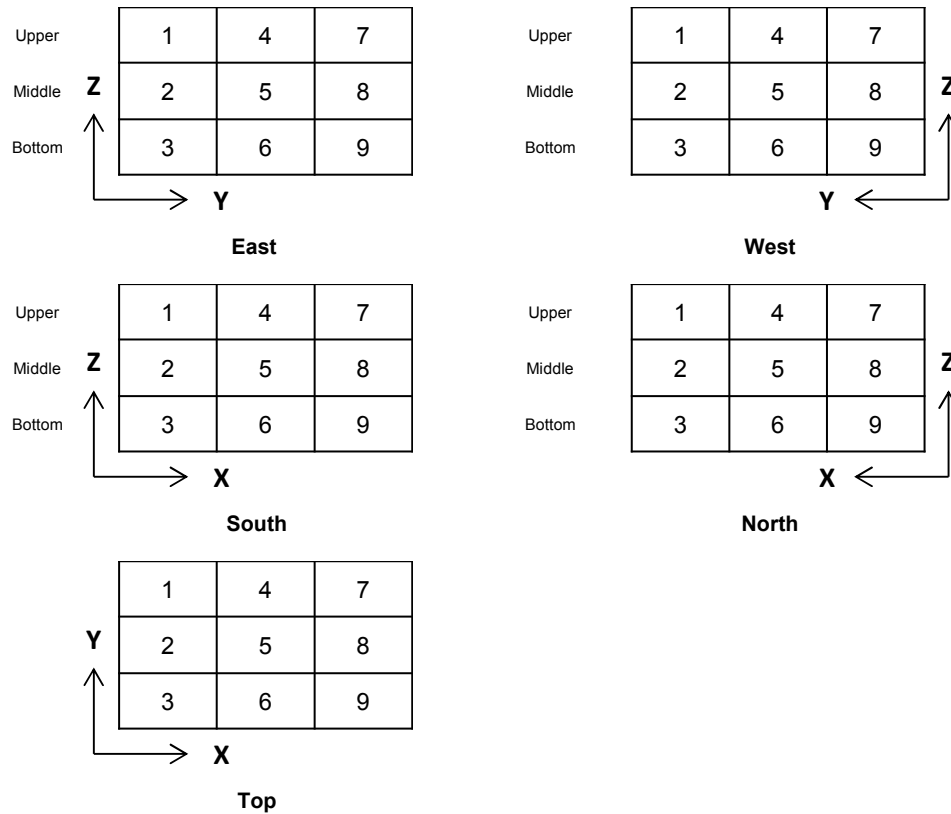


Figure 7 Pressure measurement point, numbers for locations on neighborhood surfaces

The secondary output, local wind speed, takes account of its extended use in building-scale studies by modifying the entire wind data in the TMY dataset that was initially provided as the input. Therefore, the modified TMY dataset can still represent a 30-year weather trend in an urban site, the same period when the original TMY is created. At the same time, this approach further reduces computational costs, which are the main limitation in real-time assessment of large urban areas for an entire year (Section 1.2.4).

2.2.3 TERRAIN MODEL

The proposed method employs existing terrain definitions for local wind speed,

which are used in a simple mathematical method for building simulations to represent local conditions (ASHRAE 2001, ASCE 2003). In this method, four terrain types represent various natural and built environments: unobstructed land, open land with scattered buildings, dense urban areas, and city centers with tall buildings, Table 2. For each type, atmospheric boundary layers are characterized as parameters for its thickness and wind reduction factors. These parameters are used to generate data on local wind speed at a certain height.

Table 2 Atmospheric boundary layer parameters (ASHRAE 2001)

<i>Terrain Category</i>	<i>Description</i>	<i>Wind Reduction Factors</i>	<i>Boundary Layer Thickness in Feet</i>
1 (City Center)	<i>Large city centers, in which at least 50% of buildings are higher than 24 m (8 stories or more) over a distance of at least 0.5 mi or 10 times of the height of the structure upwind, whichever is greater</i>	0.33	1500
2 (Urban)	<i>Urban and suburban areas, wooded area, or other terrain with numerous closely spaced obstructions having the size of single-family dwellings or larger, over a distance of at least 800 m or 10 times the height of the structure upwind, whichever is greater</i>	0.22	1200
3 (Industrial)	<i>Open terrain with scattered obstructions having heights generally less than 9 m, including flat open country typical of meteorological station surroundings</i>	0.14	900
4 (Unobstructed)	<i>Flat, unobstructed areas exposed to wind flowing over water for at least 1.6 km, over a distance of 4500 m or 10 times the height of the structure inland, whichever is greater</i>	0.10	700

Due to its simple usage and the empirical considerations of urban boundary layer thicknesses, which have been long developed as identified in the literature reviews (Section 1.2.4), the simple mathematical method has been widely used for a large

urban area. In particular, its negligible computational burden allows year-long analyses that are crucial for building studies (Wilson 1989).

However, the urban topographies and their effects on local wind conditions are hardly considered, regardless of their significant influences as identified in the literature reviews (Section 1.2.3). Physical wind tunnel experiments may be utilized, as they are generally acceptable to confirm the observed wind reduction factors (Simiu 2009, Niemann 1993, Cermak 1971). The associated costs in constructing a large number of mockup models with various topographies are prohibitive, while inherent errors exist, such as measuring and scaling result for building's real-life size (Duthinh and Simiu 2011, Simiu 2009).

To alleviate its weakness, wind speed from the mathematical method is calibrated with the speed database, which embeds topographic effect, preprocessed in virtual wind tunnel tests with CFD simulation. A main benefit is that using the speed database adds virtually no computational cost.

2.3 ACCEPTABLE RANGE OF ERRORS

To validate the proposed methods, acceptable ranges of errors are established to determine the prediction accuracy. Since wind data in the proposed model is generated by CFD, it is reasonable to use the same model for the precision benchmark. As the conventional method, CFD simulations use the full-scale urban geometries and materials for the territorial scope that they are used for the

proposed model. Surface wind pressure, the primary output, is validated since it also accounts for the effect of local wind speed, the secondary output.

Given that early design stages are the targeted use of the model, the error ranges are adopted from general statistical theories: 5% error being good, 10% being reasonable, but over 35% being considered unreliable (Kaye and Freedman 2000, Casella and Berger 2002, Freedman 2009). At the same time, 20% error is considered reasonable, based on the existing outdoor wind prediction researches (Blocken, Stathopoulos, and Carmeliet 2011). Therefore, the accuracy goal includes an average error of less than 20%, whereas the maximum error is less than 35%. The percentage is based on the difference from the benchmark solution, normalized by the full range of pressure (maximum – minimum) over all neighborhood surfaces within a domain of the benchmark solutions.

Since surface pressure is measured in multiple locations (45 total) as defined in Section 2.2.2, their hierarchies become the secondary accuracy goal. Hierarchies of pressure intensities are in two levels: within a surface and among other surfaces. A higher-pressure area on a surface is identified vertically and horizontally by visual representation on its pressure map, compared to the benchmark solution. The pressure values on a surface are averaged so that it can be compared with other surfaces. Thus, hierarchical pressure data can be further used as boundary conditions for smaller local-scale studies (Table 1) that need to account for surrounding contexts, a common challenge in using existing downscaling methods (Section 1.2.4).

2.4 TARGET COMPUTATIONAL EFFICIENCY

Computation efficiency is another critical measure of success. In general, the model strives to be faster than the conventional method of CFD simulation. More stringently, the run-time should be fast enough to meet the needs in the early design stages. For making decisions on at least a few design options in a day, a total run time shall be smaller than two or three hours, processing an entire year-long wind data (8760 hours) in a TMY dataset. This means that a CFD run needs to be less than 1.2328 seconds. Considering limited resources of the users, this computational goal shall be achieved with a generic personal computer, one of which is specified for the current research, Table 3. Given a small urban scale (~100 m in diameter) may take an hour (Kim, Yi, and Malkawi 2011), the model shall be 2920 times faster than a real-time CFD run for the same territorial scope.

Table 3 Computer specifications in use

<i>Processor</i>	1.8GHz Dual-Core Intel Core i7
<i>Cache</i>	4MB shared L3
<i>Memory</i>	4GB 1333MHz DDR3 SDRAM

CHAPTER 3 DATABASES AND INTERPOLATION SYSTEM

3.1 PRESSURE DATABASE

The pressure database is developed in four steps: parameterization, geometric sampling, CFD simulation, and creation of the pressure database, Figure 8. First, for computational efficiency, a complex urban context is represented with a few parameters. For data portability, the number of samples in step two is limited. In the third step, CFD simulations yield pressure data. Finally, the database is created for the sampled geometries.

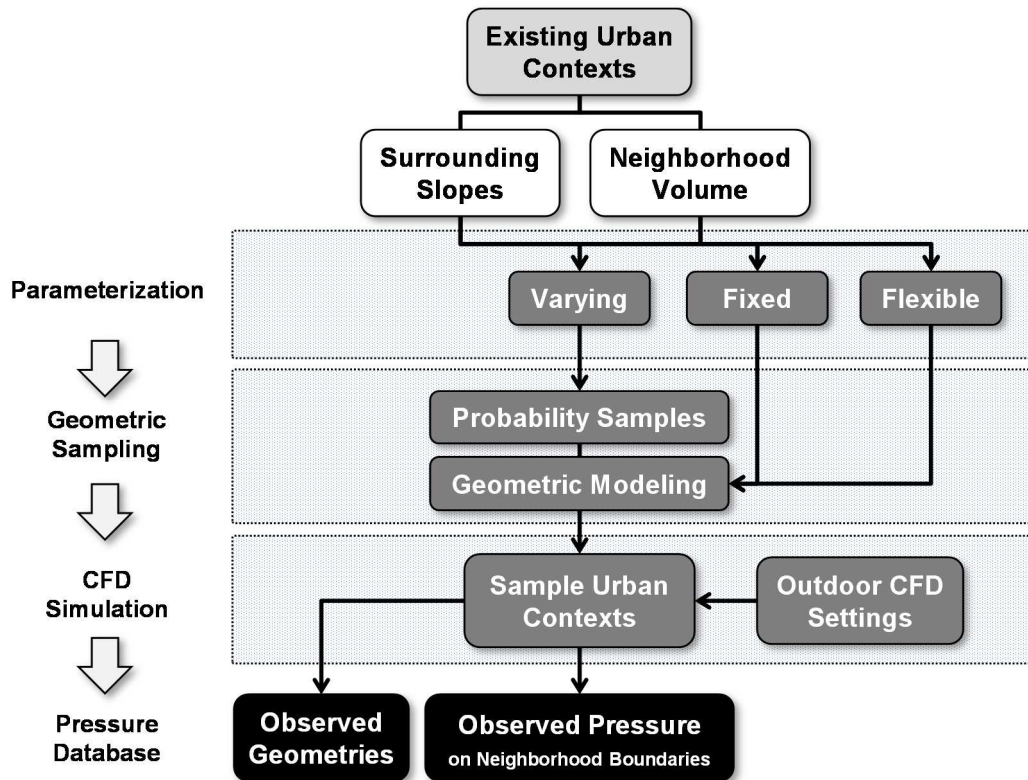


Figure 8 Pressure database with surrounding slopes and neighborhood volume

3.1.1 PARAMETERIZATION

Parameterization is the first step to represent a complex site geometry with only a few parameters. The goal is to generate geometric variants by changing the values in the parameters. For computational efficiencies, the number of parameters is minimized while the overhead operations are controlled with a CAD modeling tool. Reducing parameters also enhances the model's utilities, while facilitating other considered techniques - sampling and interpolation - since the complexities in problem domains are hence reduced.

The parameterization is adopted from computer sciences. It is a process of representing complex effects by simplified parameters, rather than computing them dynamically with the associated details (Hoare 1969). A parameter, used in a process, refers to one piece of data in an entire domain, which also includes an ordered list of overhead parameters and a set of rules to relate them. Therefore, each time a process is operated with a change in a parameter, the domain will be transformed to be another variant, whether in whole or in part.

In design and engineering practices, a parameter is a key norm of computer-aided design (CAD) modeling (Yi and Malkawi 2009, Sanguinetti and Kraus 2011, Monedero 2000). The key interest is to create new geometric families, where the members of a family differ only in dimensions, while avoiding explicit modeling of each point, line, and surface. The adjustment rules may enlist rotating, copying, moving, and scaling. These rules are applied in two types of parameters, varying, and overhead, depending how they operate. Overhead parameters include fixed

and flexible. Dimensions do not change in fixed parameters, whereas new variants are generated with varying parameters. Flexible parameters are used to generate explicitly unknown geometries with two other operations (Roller 1991, Monedero 2000, Woodbury 2010). Being the only type that is controlled by the users, the number of varying parameters is desirably minimized to generate the site geometries.

3.1.2 GEOMETRIC SAMPLING

Geometric sampling is the second step to increase computational efficiency, enabling a small number of samples to represent a whole population. This technique is critical, given that assessing an urban condition by CFD simulations requires a high computational cost, while a large number of urban conditions are needed to represent the wide range of territorial scope (Section 2.2.1) in the database.

Randomizing is a preferred sub-process, which involves probability methods for minimizing the subjectivities of chosen samples. It is used in sampling to achieve fair representation for a whole population. This is known as “probability samples” (Cochran 2007, Kaye and Freedman 2000). The proposed method uses a random-number generator for creating probability sampling points within the ranges of parameters. A uniform distribution is preferred for equal probabilities of various urban conditions in the database. The usefulness of individual samples to predict a new case is twofold: two samples can be used for numerical analyses to

interpolate what is situated in between, and a single sample can represent a new case by its geometrical similarity.

Geometric construction with a CAD tool is the next step with probability samples. Note that only varying parameters from the parameterization process are used in randomizing, while the other overhead parameters are used in geometrical construction of sample urban context.

3.1.3 CFD SIMULATION

CFD simulation is used to assess sample urban contexts for surface wind pressure that is measured at the boundaries of a neighborhood. This is done by assessing neighborhood volume and surrounding topographies. For the best practice of CFD simulations, the recommended setting for urban outdoor environments are summarized below, while CFD capacities and limitations were overviewed in Section 1.2.4.3

The computational domain size is based on wind engineering recommendations for urban pedestrian environments, which were successfully cross-referenced with wind tunnel experiments and field measurements (Tominaga et al. 2008, Franke 2006). The lateral and top boundaries are away from the target building. They are set at more than 5 times the neighborhood height ($5H$), while inlet and outlet boundaries are at least $10H$ away from the nearest surface of the neighborhood.

For the turbulence model, the Reynolds Averaged Navier-Stokes (RANS) model is used for its known validity, with K-epsilon Renormalized Group (RNG) for added accuracy on pressure and velocity (Wilcox 1998). A pressure-based solver with steady state setting is used with the standard gravitational acceleration of the earth in 9.80665 m/s^2 . For the numerical approximation, the second order upwind is used to increase accuracies in momentum, gradient, pressure, turbulent kinetic energy, and turbulent dissipation rate (ANSYS 2009).

For meshing, triangular and tetrahedral cells are chosen for surfaces and volumes respectively, because of their easiness in meshing for three-dimensional objects, regardless of their complexities. For solving boundary layers efficiently, prism layers are added on the neighborhood surfaces. The maximum change in grid spacing is equal to or smaller than 20% for smoothness in changes of cell sizes (ANSYS 2009, Bern and Plassmann 1997). The number of individual cells on any wall surface is minimum 1/10 of the building scale to reproduce separation flow around building corners (Franke 2006). These recommended settings are applied through the dissertation both in creating the database for the model and the benchmark solution for the evaluation.

3.1.4 PRESSURE DATABASE

The pressure database is created with the two sets of data from the previous processes: the sampled parameters and their pressure data. The sampled parameters represent variants of urban conditions, whose pressures are assessed

with CFD simulation. These two sets of data represent the “observed” cases, which are used to predict the “unobserved” (new) cases with support of interpolation technique described in the next step. As a limit of the method, a parameter of an unobserved case needs to be within the range of the database for the observed cases. Therefore, a range of parameters needs to be carefully defined for various urban conditions that may interest the users.

The major benefit of using a database is to save computational cost, which otherwise has to be spent for real-time CFD runs. The computer resource is needed just for numerically analyzing the characteristics of parameters in the database and for acquiring their associated pressure data. Due to the characteristics of samples in the database, the outcome is spatially sensitive, which was identified as a shortcoming in the boundary condition of existing models in Section 1.2.4.3.

The portability of the database is also considered because of limited resources that a user may have in the early stage of the design process. Hence, the number of samples needs to be minimized as long as the accuracies stay reasonable. This is the main reason why the model test is initially begun with a small number of samples in Chapter 4. At the same time, it is desirable to minimize the number of parameters for each sample since they directly affect the size of the database. Additionally, the number of measurement locations for surface pressure can be minimized, although they should be enough to show the intensity hierarchies, as identified in Section 2.2.2.

3.2 SPEED DATABASE

The speed database is developed in three steps: geometric sampling, CFD simulation and reduction ratio, Figure 9. The resultant reduction ratio for existing urban contexts considers terrain and slope by using the existing mathematical method and CFD simulations.

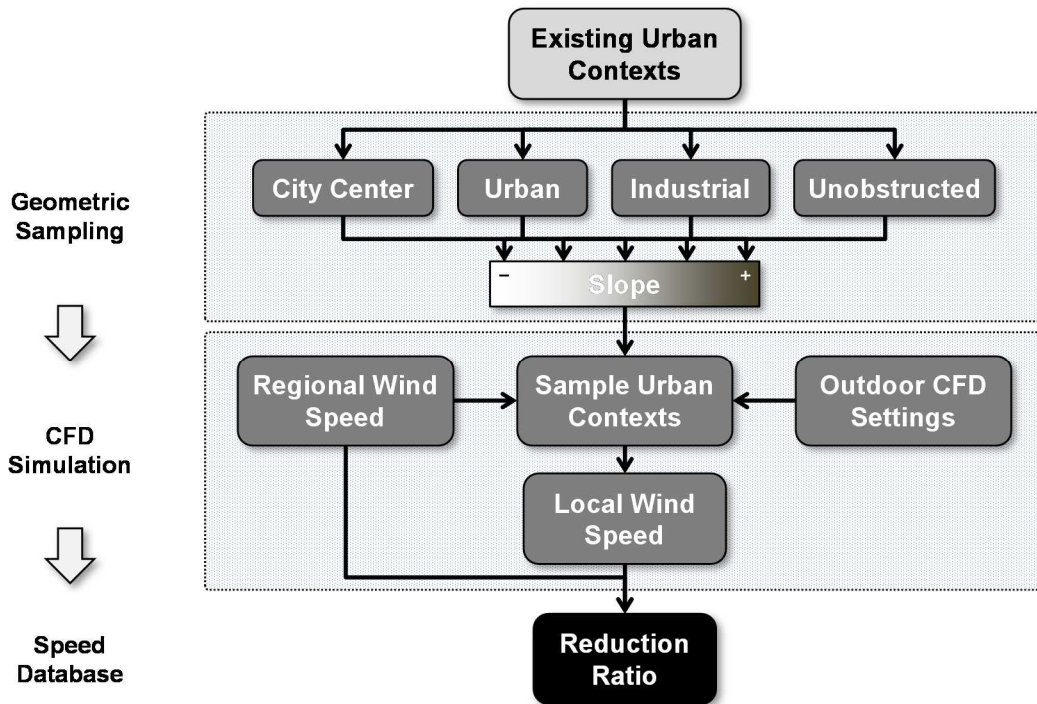


Figure 9 Speed database with terrain and slope

3.2.1 GEOMETRIC SAMPLING

The first step is geometric sampling. Samples of terrain and slope are generated for existing urban contexts. Terrain includes buildings and streets, geometrically built based on the existing mathematical model (Section 2.2.3), which enlists four

(4) types depending on the size and density of buildings in a region: city center, urban, industrial, and unobstructed. Positive or negative slope is added to generate the variants of each terrain.

3.2.2 CFD SIMULATION

As the second step, to assess the effect of the geometric samples on local wind speed, CFD simulation is conducted. Each terrain is evaluated for how it obstructs outdoor wind flow along with topographic effect of slopes. As inlet velocity, a regional wind speed is acquired from a TMY dataset, while localized wind speeds are measured at outflow locations in the domain. Boundary conditions are consistent among different terrain types, for building materials, CFD settings, and the territorial scope. The recommended settings for the outdoors are adopted as in the pressure database (Section 3.1.3).

3.2.3 REDUCTION RATIO

The third step is to identify the reduction ratios in wind speeds incurred by each terrain on a slope. This is done using CFD simulations. This process begins with inspecting the simulation result to understand the impact of terrain and topography on wind patterns. By analyzing result data, an urban condition on a slope is correlated with its impact on downscaling the ratio between input regional wind speed and its local counterpart. The reduction ratio will be used in the interpolation process, particularly for calibrating the existing mathematical method. Hence, the

real time use of CFD simulations can be avoided, enhancing computational efficiency of the model for the early design stages, while better representing the urban context with both terrain and slope.

3.3 INTERPOLATION

To predict wind pressure for a new urban context, the proposed interpolation system has two components: pressure approximation and refinement with speed, Figure 10. The initial pressure is approximated using the geometry and the pressure data from the pressure database. The initial pressure is refined with the reduction ratio from the speed database to account for terrain influences.

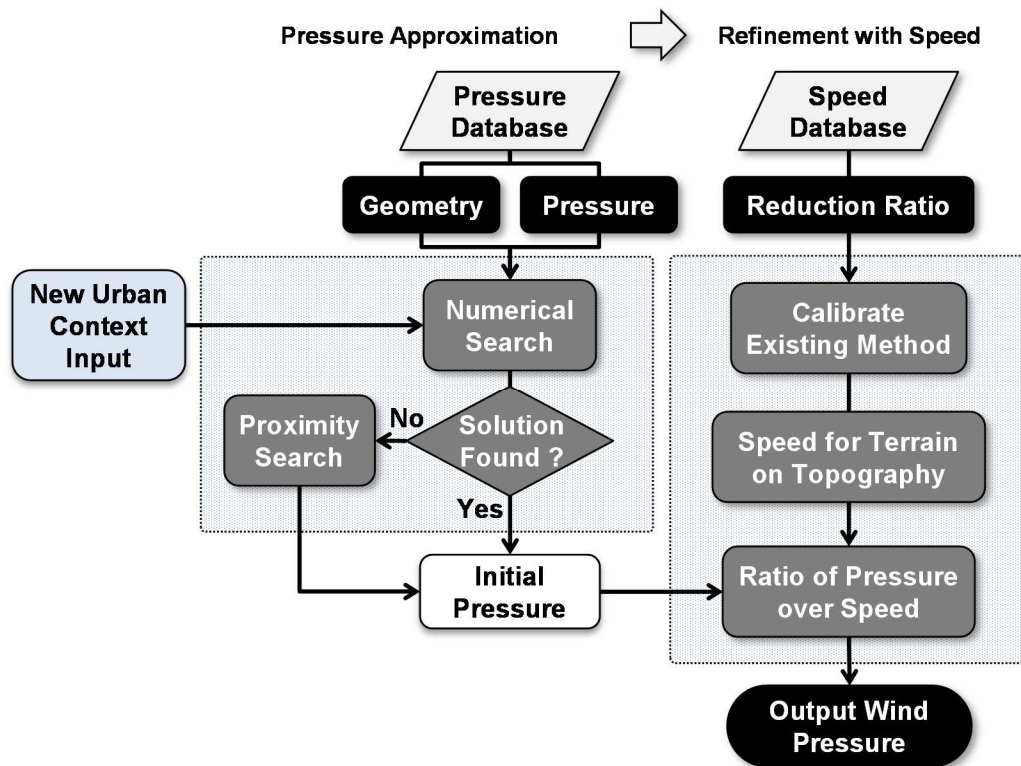


Figure 10 Interpolation system with pressure and speed database

Interpolation is adopted from engineering and science for computational efficiency; the method uses the analyses of sample data instead of solving complex mathematical functions (Bulirsch and **Stoer** 2002). Due to inherent approximations in interpolation, errors are inherent, depending on problem domains, number of samples and their robustness, and interpolation methods. However, the benefit in computational lightness and comprehensibility of complex system is far greater than the resultant loss in accuracy (Kahaner, Moler, and Nash 1989, Hamming 2012).

3.3.1 PRESSURE APPROXIMATION

The first step is pressure approximation to predict the initial pressure for a new urban context input. A numerical search (triangulation-based) model is chosen because the pressure database has no particular patterns among samples, due to the randomized sampling method. The sample data points, represented by parameter values, are connected to create triangle surfaces that allow linear interpolating for new cases. “Delaunay triangulations,” in particular, are known for minimal skewedness by maximizing minimum angles in the construction of triangles, a method commonly used in geo-statistical research (de Berg et al. 2008). This technique is also appropriate for high-dimensional problems, such as those in the current research (Simionescu and Beale 2004, Iyer and Watson 2006).

Even if a numerical search model is preferable for its reasonably high prediction accuracy, it does not guarantee a solution. Therefore, another high-dimensional

interpolation model, known as “proximity search” is also employed (Zezula et al. 2006). Proximity search evaluates the characteristics of individual samples in a database, to find the most similar one and acquire its associated pressure data as output. Hence, the proposed method takes advantages of both models, primarily by using the numerical search for a high accuracy, and successively by using proximity search to ensure a solution if the numerical search did not provide one.

3.3.2 REFINEMENT WITH SPEED

3.3.2.1 CALIBRATING THE EXISTING METHOD

The initial pressure from the pressure approximation is refined with speed for the outcome wind pressure. With the speed database, the first step is to generate local wind speed data by calibrating the existing method. Local wind speed, assuming a terrain on a flat site, is first calculated by the mathematical method, with a regional wind speed from a TMY dataset. The difference between the local and the regional wind speed is adjusted with the reduction ratio in the database, which account for terrain and slope. As a result, wind speed is reduced more (or less), due to the added topographic effect, for the existing atmospheric boundary layer parameters for each terrain (Table 2).

One of the capacities of the existing mathematical method is to generate a vertical wind profile that has varying wind speeds for different heights, considering the effect of each terrain. For simplification, however, the reduction ratio uniformly applies to any measurement height. As an example for urban terrain, a regional

wind speed of 10 m/s is downscaled to be a local speed of 7.20 m/s at the height of 10 m above ground. It is further reduced to be 6.26 m/s, by applying the normalized reduction ratio of 1.34 for a slope in 1/10. For the same terrain, at 20 m above ground on the other hand, the existing mathematical method predicts a local wind speed of 8.39 m/s, which becomes 7.84 m/s by calibrating with the same ratio.

3.3.2.2 RATIO OF PRESSURE OVER SPEED

Refining the available surface pressures from the pressure database with the calibrated local wind speed is the second step. This process adds the influence of surrounding terrains (Section 3.2) to surface wind pressures that accounted for surrounding slopes (Section 3.1). The resultant pressure is the outcome of the entire proposed method, as one of the prediction goals.

For quick assessments of buildings' surface pressure, an analogical scheme is adopted, which is widely used in building simulations: a constant ratio of pressure over wind ($\frac{\text{Pressure}}{\text{Speed}^2}$). It is derived in a semi-empirical approach, from the building airflow experiments and Bernoulli's equation (Dyrbye and Hansen 1997, ASHRAE 2009, Hensen and Lamberts 2012). This analogical scheme is modified to (1) for the given problem.

$$\frac{P_{obstructed}}{U_{obstructed}^2} = \frac{P_{unobstructed}}{U_{unobstructed}^2} \quad (1)$$

Where $P_{obstructed}$ is surface pressure with a terrain with obstructions on a sloped site, and $U_{obstructed}$ is local wind speed at the height where $P_{obstructed}$ is measured. In contrast, $P_{unobstructed}$ is surface pressure with unobstructed terrain on a sloped site, and $U_{unobstructed}$ is local wind speed at the height where at $P_{unobstructed}$ is measured.

Equation (1) compares a ratio of pressure and speed in a terrain condition to another ratio for unobstructed terrain. $P_{unobstructed}$ and $U_{unobstructed}$ represent surface wind pressure on neighborhood boundaries and local wind speed, both of which are downscaled with the unobstructed terrain on a sloped site. When there is a change in either terrain or slope, both wind speed ($U_{obstructed}$) and surface pressure ($P_{obstructed}$) have to change to keep their constant ratio. To better suit the current problem of solving $P_{obstructed}$, (1) is transformed to (2).

$$P_{obstructed} = \left(\frac{U_{obstructed}}{U_{unobstructed}} \right)^2 * P_{unobstructed} \quad (2)$$

This unknown variable, $P_{obstructed}$, is solved with the other known variables: local wind speeds for the obstructed and unobstructed terrain, as well as surface wind pressure in the unobstructed terrain. The approximation with pressure database provides $P_{unobstructed}$, whereas $U_{obstructed}$ and $U_{unobstructed}$ come from calibrating the existing method with the speed database. The known variables are generated under a certain slope. As a result, $P_{obstructed}$ represents the primary outcome of the model; it shows surface wind pressure on a neighborhood boundary by comprehensively accounting for a surrounding urban condition, including buildings and topography.

CHAPTER 4 PRESSURE DATABASE DEVELOPMENT

This chapter develops the pressure database with the proposed model and its employed techniques. For data portability, a small number of urban context samples are initially generated and evaluated; accuracy is improved by adding more samples until the prediction goals are met. More tests are conducted for different volumes of neighborhood to gain confidence in the model's accuracy. Then the proposed method is finally tested for its sensitivity and how well it conforms to existing studies.

4.1 INITIAL DATABASE WITH 11 SAMPLES

Only a handful of samples are generated in the initial database. The number is small in comparison to numerous possible samples, which are required to cover the urban area of interest (Section 2.2.1). Thus, the size of the database can be minimized for portability, while total computation resources can be saved to assess samples with CFD simulation at the same time. Since there is no clear theory to determine the minimum number of samples, eleven (11) samples are initially generated and tested. If necessary, more samples are added for higher accuracy, while observing the associated computational cost.

4.1.1 PARAMETERIZATION OF SITE GEOMETRY

For parameterization, a simple site geometry is defined, using overall symmetries in aerial view. Four surrounding slopes constitute a topographic condition, along with the extruded square shape for neighborhood volume as shown in Figure 11.

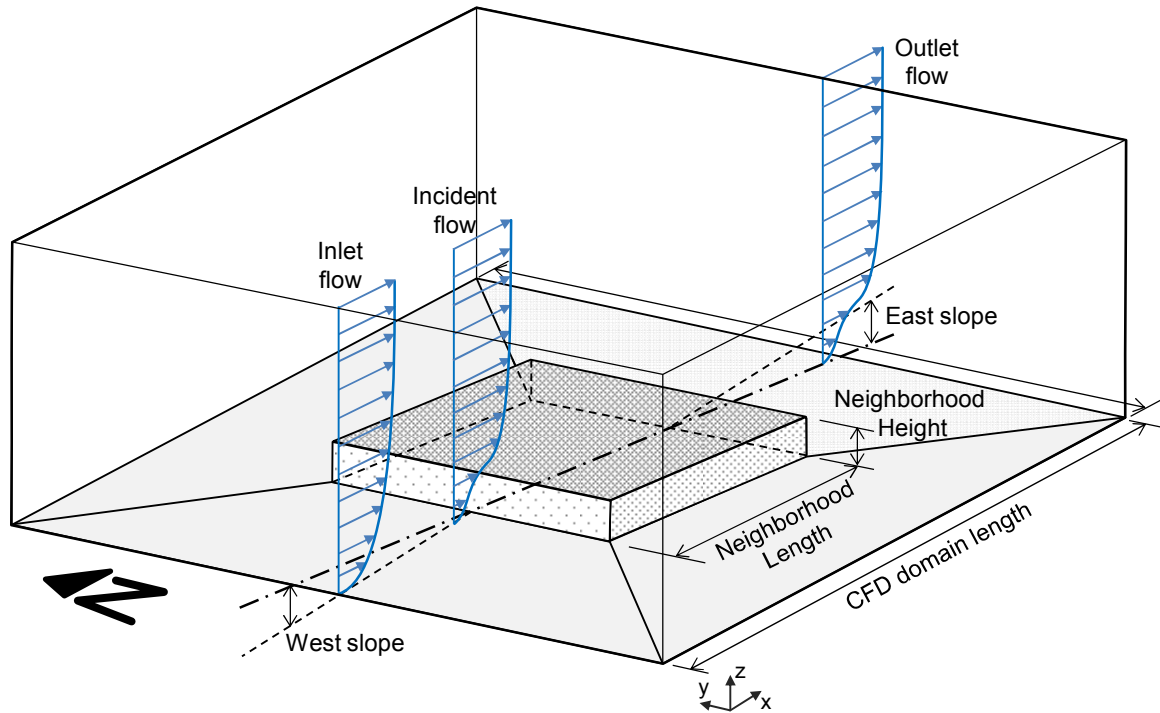


Figure 11 Parameterization of site geometry with slope and neighborhood volume

To generate variants of the topographic condition, three types of geometry are sub-defined, based on the parameterization technique: varying, fixed, and flexible. The varying parameter includes the west and east slopes for the steepness of topographies, and the height and length of a neighborhood volume. The fixed parameter includes the length and width of the entire computational volume for the

CFD simulation. The flexible parameter includes the width of neighborhood and slopes of north and south, which are generated with other two type of parameters.

With varying parameter changes, a set of adjustment rules is applied to create a flexible geometry, such as generating lines by connecting points among the varying and the fixed. These lines consequently become the base information to generate surfaces. To execute the rule sets, a recent tool development (McNeel 2010) with Non-Uniform Rational B-Splines (NURBS) is adopted.

By applying a parameterization technique, slopes on the east and west represent the dominant, while others on the north and south are the subsidiaries. If the dominant slope is on the north-south axis, the geometry can be simply rotated by 90° since the shape of the entire domain and neighborhood volume is square in the aerial view. The proposed parameterization scheme can generate major topographic variations: flats, hills, and valleys. Their combinations can be also made by adjusting dominant slopes independently, such as a downslope on one slope but a flat on another.

4.1.2 RANGE OF PARAMETERS

For generating variants of the defined site geometry, the ranges of each parameter are defined for the urban scale of interest, beginning with the varying parameters. Regarding neighborhood volume, length (equal to flexible parameters of width) varies between 100m and 500m, based on the neighborhood scale explained in

Section 2.2.1. Neighborhood height varies between 9m and 60m, representing 3 to 20 story buildings that may cover major portions of a city in the United States (U.S.). For illustration, this is equivalent to more than 90% of buildings in Los Angeles (California), Phoenix (Arizona), and Salt Lake City (Utah) (Ratti 2002).

The slopes, another varying parameter, represent immediate topographies that are most influential in an urban site. The range of slopes varies from $+1/10$ to $-1/10$, covering typical city areas in the US. It is determined based on existing indicators, even if there is no statistical data for all urban conditions and such extensive surveys are not feasible. The first indicator, the Americans with Disabilities Act (ADA), mandated that $1/12$ is the maximum slope for man-powered vehicles and low powered vehicles, and $1/10$ slopes are allowed with handrails (Becerra 2010). The second indicator is that existing slopes in U.S. cities are affected by American Association of State Highway and Transportation Officials regulations (AASHTO). AASHTO states that legal urban streets shall be less than $1/6.6$ (15%) incline, and residential areas shall have a maximum of $1/8.3$ (12%) incline and preferably $1/12.5$ (8%) for main walking directions (AASHTO 2001). Therefore, $(+/-) 1/10$ is a reasonable range of slopes for the current study.

The ranges of flexible parameters are governed by the varying parameters for their geometrical hierarchies, defined in Section 3.1.1. Even if a subsidiary slope may have different shape from a dominant one, the dimensional limits are the same since they are bound by the same fixed parameters.

The ranges for fixed parameters are chosen to represent a region, where the width and length of a CFD domain are 1000 m. The height of a CFD domain is determined based on the recommendation for outdoor urban area (Section 3.1.3), ensuring that the distance to the top of the neighborhood volume is more than 5 times the height of the actual neighborhood. The lateral and top boundaries are away from the target building, more than 5 times the neighborhood height (5H). The ranges of parameters are summarized in Table 4.

Table 4 Range of parameters for neighborhood size and topography

	<i>Varying parameters</i>				<i>Flexible parameters</i>		<i>Fixed parameters</i>		
	<i>Neighborhood length</i>	<i>Neighborhood height</i>	<i>West slope</i>	<i>East slope</i>	<i>North slope</i>	<i>South slope</i>	<i>CFD domain width</i>	<i>CFD domain length</i>	<i>CFD domain height</i>
<i>Minimum</i>	100 m	9 m	-1/10	-1/10	-1/10	-1/10	1000 m	1000 m	500 m
<i>Maximum</i>	500 m	60 m	1/10	1/10	1/10	1/10			

Apart from the geometrical parameters, another varying parameter - wind speed - is added. Its range is from 0 to 10 m/s, which covers most normal wind conditions for Detroit MI, Philadelphia, PA, Los Angeles, CA, Chicago, IL, Tampa, FL, New York, NY and many other U.S. cities, based on TMY3 data summarized at Figure 12. With the added variable, the interpolation model can predict varying surface pressure without having to CFD simulate the same site geometries with multiple wind speeds, by taking advantage of the simple relation between wind speed and surface pressure, commonly used for building-scale airflow experiments (Dyrbye and Hansen 1997, ASHRAE 2009).

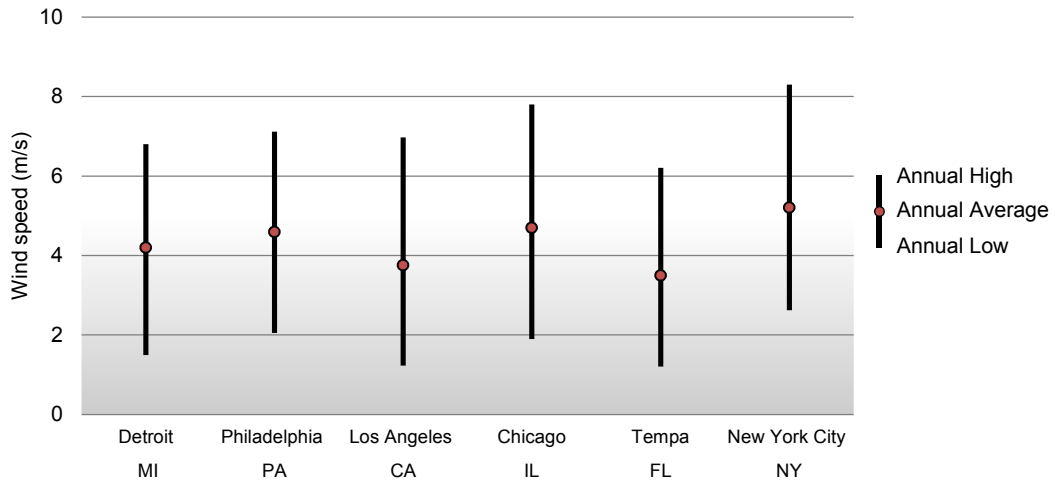


Figure 12 Range of regional wind speeds in U.S. cities (m/s)

4.1.3 SAMPLING WITH VARYING PARAMETERS

With the defined range, urban site geometries are generated based on the geometric sampling technique (Section 3.1.2). For the 11 samples and the 5 varying parameters, a two-dimensional matrix (11 by 5) is first filled with random numbers between 0 and 1, in a uniform distribution, for which a MATLAB function is employed. These numbers are then scaled for each parameter range, shown at the Table 5, which becomes one part of the database. Two other parameters are excluded for their overhead role, which is effective only for generating geometries in the NURBS modeling tool. Figure 13 illustrates the generated sample geometries with sample IDs, corresponding to Table 5, with various volumes and topographic conditions.

Table 5 Varying parameters for sample site geometries in the database

Sample ID	Neighborhood length (m)	Neighborhood height (m)	West slope	East slope	Wind speed (m/s)
1	425.8	28.9	-1/11	1/200	0.3
2	210.8	36.5	-1/15	1/37	5.6
3	456.4	59.1	1/30	-1/32	4.4
4	327.6	25.6	-1/14	1/40	10.0
5	204	28.7	1/20	1/11	5.2
6	412.2	43.6	1/22	-1/500	1.2
7	294.8	45.8	-1/24	1/22	1.7
8	462	47.5	1/18	-1/33	5.0
9	371.6	17.5	-1/15	-1/19	7.1
10	422.2	53.1	-1/13	1/111	2.4
11	169.4	41.1	-1/13	1/67	0.1

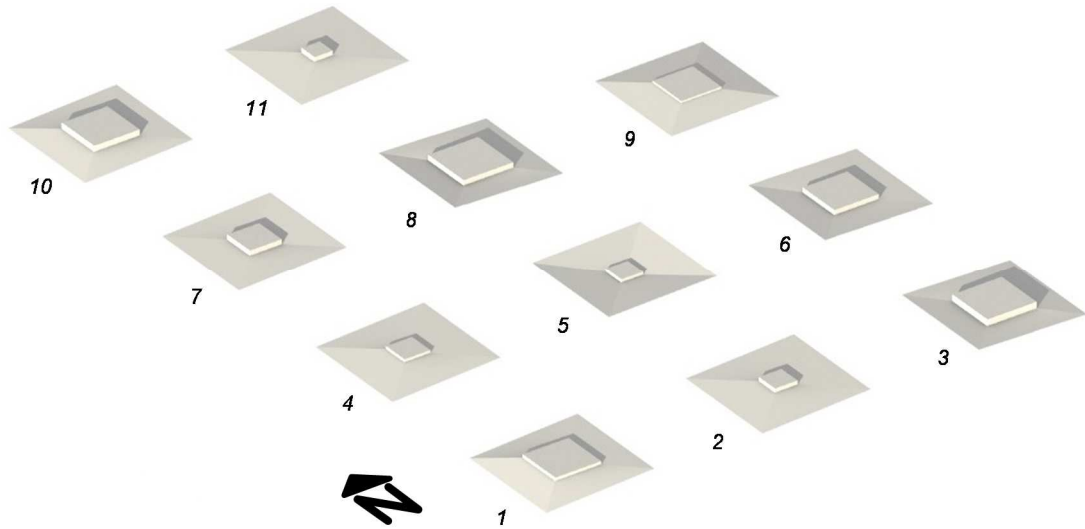


Figure 13 Sample site geometries for CFD simulations

4.1.4 WIND PRESSURE ASSESSMENT FOR SAMPLES

Surface wind pressure data is prepared in Table 6, by assessing each of the sample site geometries that are generated from the sampling process. In CFD

Table 6 Wind pressure data for the sample site geometries (Pascal)

		<i>Sample ID</i>										
		1	2	3	4	5	6	7	8	9	10	11
<i>North</i>	1	101325	101320.8	101321.6	101325.8	101324.7	101325	101324.4	101320.7	101323.5	101324.6	101325
	2	101325	101319.8	101321.1	101326.9	101324.4	101325	101324.4	101320.5	101323.8	101324.5	101325
	3	101325	101318.8	101321	101329.3	101324.3	101325	101324.4	101319.8	101324	101324.5	101325
	4	101325	101325.5	101327.1	101327.2	101325.5	101325.1	101325.1	101326.3	101327.2	101325.5	101325
	5	101325	101325.5	101327.2	101327.5	101325.6	101325.1	101325.1	101326.3	101327.2	101325.5	101325
	6	101325	101325.8	101327.2	101327.1	101325.7	101325.1	101325.1	101326.5	101327.1	101325.5	101325
	7	101325	101326	101326.6	101326.8	101325.4	101325.1	101325.1	101325.7	101326.8	101325.5	101325
	8	101325	101325.9	101326.6	101327.2	101325.4	101325.1	101325.1	101325.8	101326.7	101325.5	101325
	9	101325	101326	101326.4	101325.5	101325.4	101325	101325.1	101325.5	101326.6	101325.4	101325
<i>East</i>	1	101325	101338.5	101343.7	101343.3	101332.2	101326.1	101326.5	101345	101342	101328.3	101325
	2	101325	101340.3	101348.8	101342.4	101332.9	101326.2	101326.5	101352.3	101357	101329.7	101325
	3	101325	101340.7	101349.9	101342.9	101333.1	101326.2	101326.6	101352.6	101359.4	101330	101325
	4	101325	101337.9	101347.6	101349.3	101332.5	101326	101326.4	101347.4	101353.9	101329.1	101325
	5	101325	101342.2	101351.1	101352.8	101333.2	101326.3	101326.6	101353.7	101359.9	101330.1	101325
	6	101325	101342.7	101351.8	101355.4	101333.1	101326.3	101326.6	101354.7	101363.4	101330.3	101325
	7	101325	101338.2	101342.9	101341.3	101330.7	101326	101326.3	101347.1	101358.1	101329.2	101325
	8	101325	101341.2	101349.3	101346.7	101331.7	101326.2	101326.5	101352.2	101362.3	101329.8	101325
	9	101325	101341.1	101350.3	101346.6	101331.7	101326.3	101326.5	101352.5	101365.7	101330	101325
<i>South</i>	1	101325	101326.6	101326.5	101327	101325.6	101325.1	101325.2	101326.2	101326.3	101325.5	101325
	2	101325	101326.6	101326.5	101326.8	101325.6	101325.1	101325.2	101326.1	101326.4	101325.5	101325
	3	101325	101326.7	101326.3	101326.3	101325.6	101325.1	101325.2	101326	101326.3	101325.5	101325
	4	101325	101325.5	101327.1	101327	101325.5	101325.1	101325.1	101327	101326.6	101325.4	101325
	5	101325	101325.6	101327.2	101327	101325.6	101325.1	101325.1	101327	101326.3	101325.4	101325
	6	101325	101325.5	101327.3	101326.6	101325.6	101325.1	101325.1	101326.8	101326.6	101325.4	101325
	7	101325	101322.7	101321.3	101328.6	101324.5	101324.9	101324.6	101322.5	101323.8	101324.5	101325
	8	101325	101323.2	101320.6	101328.9	101324.2	101324.9	101324.6	101323	101323.4	101324.6	101325
	9	101325	101322.5	101321.6	101329	101324	101324.9	101324.7	101322.3	101323.6	101324.4	101325
<i>West</i>	1	101325	101324.1	101324	101327.1	101323.5	101324.9	101324.9	101320.8	101317.5	101324.1	101325
	2	101325	101323.7	101324.1	101327.1	101323.8	101324.9	101324.9	101322.8	101317.3	101324.5	101325
	3	101325	101323.7	101324.1	101323.8	101323.8	101324.9	101325	101323.3	101317.6	101324.7	101325
	4	101325	101326.1	101325.9	101321.4	101325.4	101324.9	101325	101324.3	101314.7	101325	101325
	5	101325	101326.7	101326.2	101320.9	101325.3	101324.9	101325.1	101325	101315.8	101325.1	101325
	6	101325	101326.9	101326.3	101320.9	101325.3	101325	101325.1	101324.9	101315.8	101325.2	101325
	7	101325	101325.4	101323.1	101326.6	101324	101324.9	101325.1	101321	101316.5	101325.5	101325
	8	101325	101325.5	101324.1	101326.6	101324	101324.9	101325.2	101322.3	101316.3	101325.6	101325
	9	101325	101325.6	101324.2	101323.9	101324	101324.9	101325.1	101322.8	101316.3	101325.6	101325
<i>Top</i>	1	101325	101326.1	101325.9	101325.5	101325.5	101325	101325.1	101325.6	101324.7	101325.4	101325
	2	101325	101326.6	101325.9	101324.6	101325.6	101325.1	101325.2	101326.2	101324.9	101325.3	101325
	3	101325	101326.5	101325.9	101325.4	101325.6	101325.1	101325.2	101325.4	101324.8	101325.5	101325
	4	101325	101324.5	101325.8	101326.4	101325.2	101325	101325.1	101325.6	101325.5	101325.3	101325
	5	101325	101325	101325.2	101325	101325.3	101325	101325	101325	101325	101325	101325
	6	101325	101325.2	101326.3	101325.7	101325.3	101325.1	101325	101326.2	101326	101325.2	101325
	7	101325	101319.7	101319.6	101282.1	101323.5	101324.7	101324.7	101320.4	101320.6	101324.2	101325
	8	101325	101320.2	101316.8	101267.7	101319.8	101324.7	101324.6	101317.3	101319.6	101324.3	101325
	9	101325	101321.5	101318.9	101281.2	101323.4	101324.8	101324.5	101319.4	101320	101324.3	101325

domains, the inlet wind flow progresses from the west for all samples, while its speed is acquired from the defined varying parameter (Table 4). Measurement locations (9 points on each surfaces) are based on the targeted output in Section 2.2.2. This set of pressure data completes the database of the initial case study, along with the varying parameters. For CFD simulations, one of the commercially available packages, ANSYS FLUENT 14, is used for its text-based control that allows setting a large number of simulation runs.

4.2 INITIAL INTERPOLATION TEST

Utilizing the initial database with 11 samples, one test case was set to observe the prediction accuracy and computational efficiency with the proposed interpolation method (Section 3.3). The test case contains a neighborhood volume of 30 meters in height and 200 meters in length, which sits on a mixed-slope topography, with a positive slope on the east and a negative slope on the west. Wind speed of 3.4 m/s comes from the west, the same direction for the prepared database (Table 6). The parameters for the prediction test are summarized at Table 7. The test site geometry is shown in Figure 14, showing the tags a, b, c, and d to help identify the surface orientations for the prediction results.

Table 7 Parameters of the urban condition for prediction test

Neighborhood length (m)	Neighborhood height (m)	West slope	East slope	Wind Speed (m/s)
200	50	-1/20	1/10	3.4

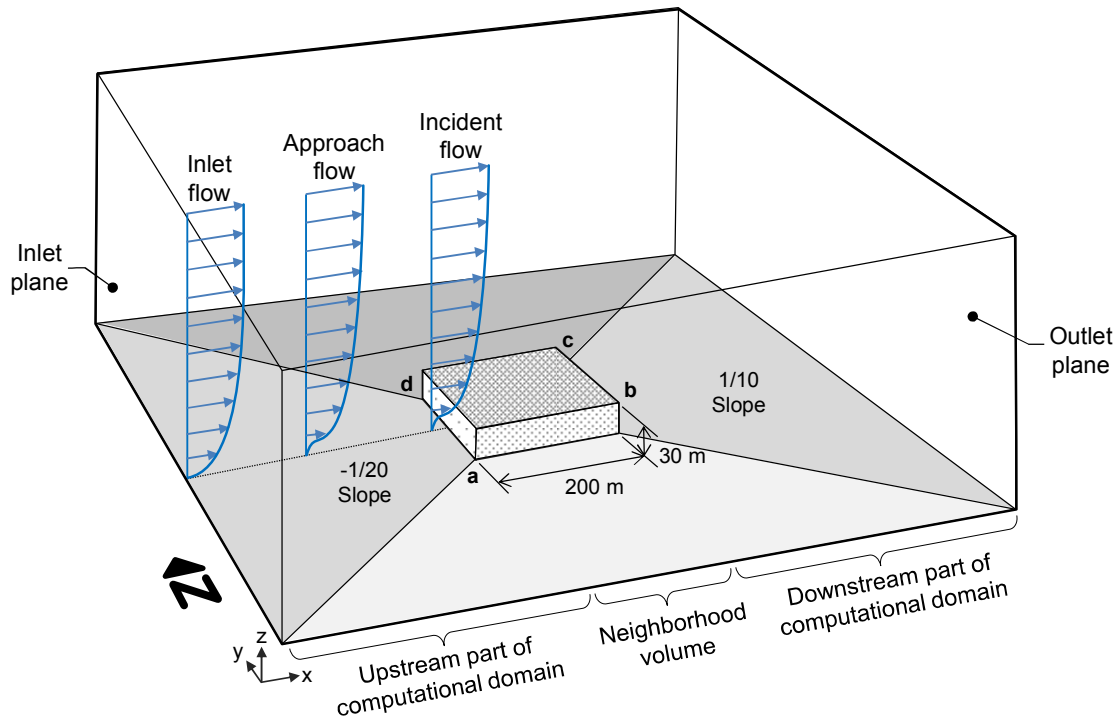


Figure 14 Site geometry with mixed-slope for initial prediction testing

For pressure approximation, a MATLAB function “Griddatan” is chosen as the numerical search model, for its prediction robustness and computational efficiencies (Filipova and Hajovsky 2011). Griddatan uses the Delaunay triangulation, identified in Section 3.3.1, for the current high-dimensional problem with no particular patterns among samples. Proximity search model is currently excluded for simplification.

The initial test results are shown at Figure 15, which compares the pressure maps by the proposed method and by the full-scale CFD simulation. The lighter shades indicate the higher pressures, with the arrows to the lowest area. The north surface is excluded because its outcome is very similar to the south surface.

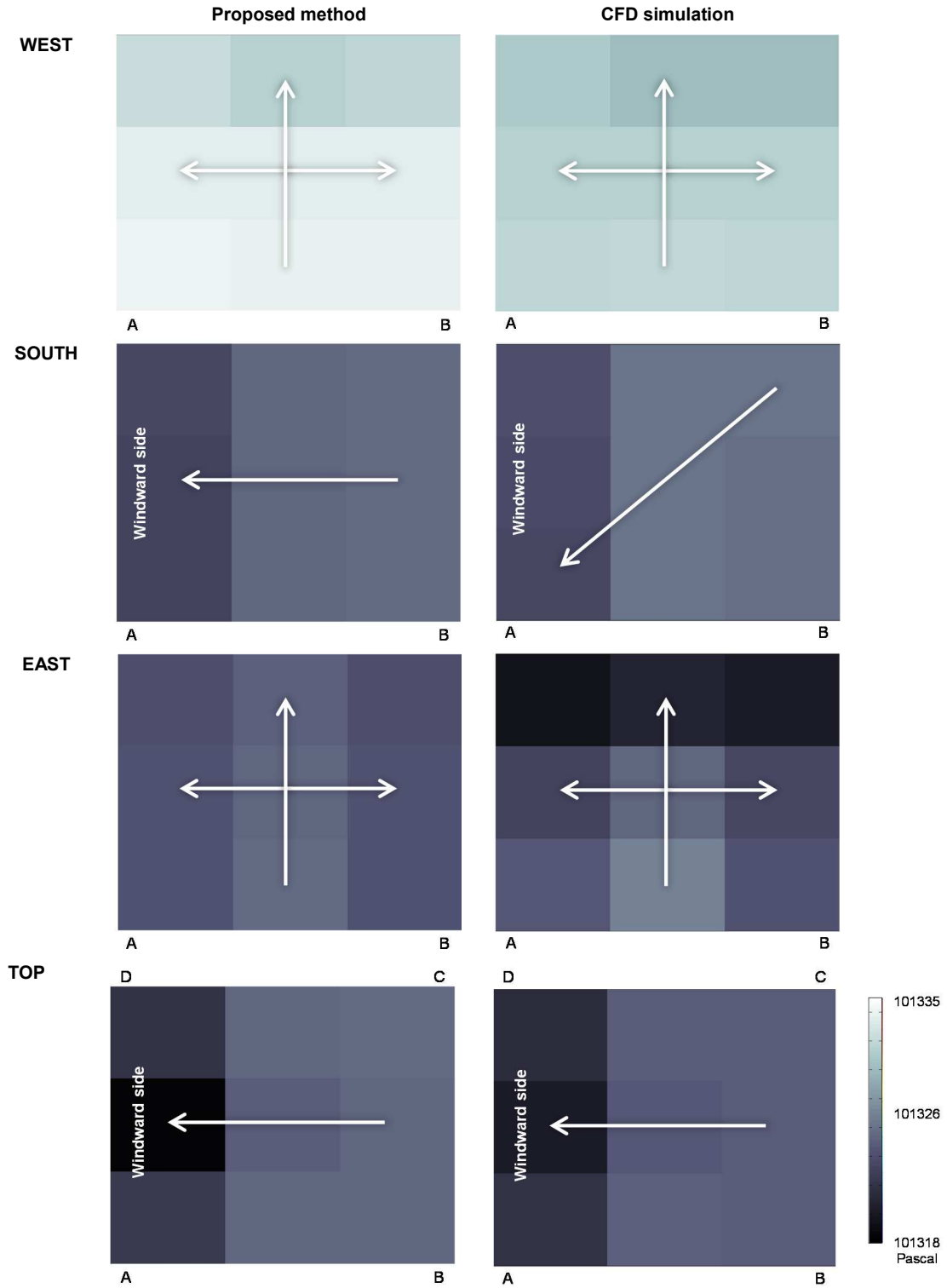


Figure 15 Initial test result with small number of samples for pressure database (Pascal)

Most notably for all individual surfaces, the directions of pressure intensities show good agreements. The south surface is the only one that shows a discrepancy in the vertical direction, showing a partial success in pressure hierarchy within a surface. This may result from the interpolation uncertainties with the small number of samples.

For pressure hierarchy among surfaces, the result of the initial test is plotted at Figure 16. The highest average pressure is found on the west surface, both by the proposed method and by the CFD simulation. This is because of its windward condition that faces against the progression of wind flow. The difference to the second highest is by 10.18 Pascal on south surface has and there is no significant difference to other two surfaces, east and top, respectively, varying by 0.12 and by 1.20.

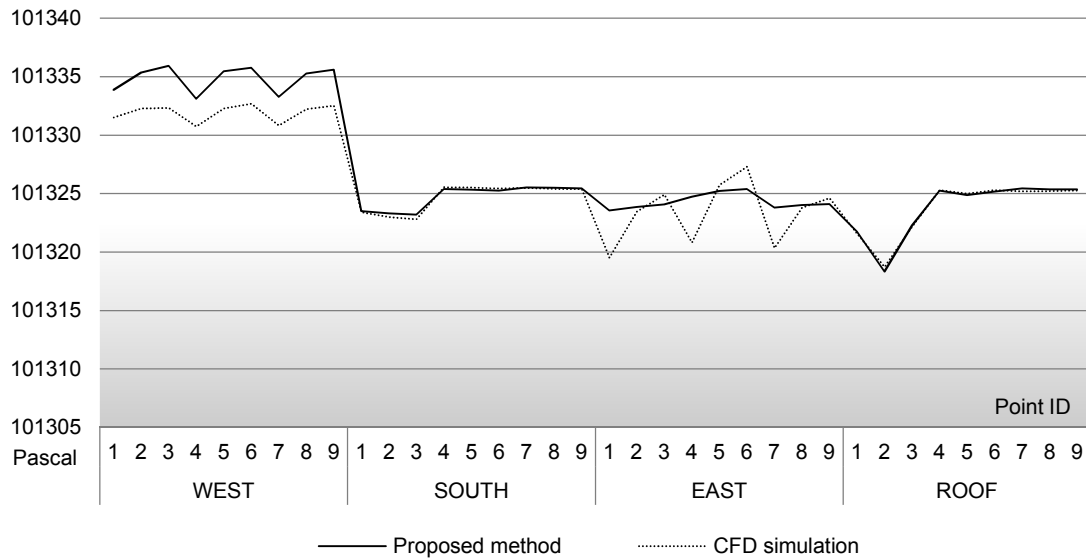


Figure 16 Initial test result at each point of the surfaces (Pascal)

On the other hand, a discrepancy was found regarding the east surface that is in a leeward condition. While this average intensity is the third highest in the predicted solution, it is the fourth highest among surfaces analyzed by the CFD simulation. This is due to the over-predictions on the lower portion of the surface (point ID of 1, 4, or 7 in the figure), for which accuracy improvement becomes necessary.

The initial prediction errors are analyzed at Table 8. The average errors of each surface, except for the west, are roughly smaller than 15%. This is within the reasonable range, but is noticeable because only eleven samples were used. However, the error range on the west surface is unreliable by 52.51 up to 68.65%, and on the east surface by -16.11 up to 52.34%. The problematic surfaces with a partial success warrant more examinations that focus on observing problematic surfaces in a windward and a leeward condition.

Table 8 Normalized errors in initial model prediction (%)

	<i>Maximum</i>	<i>Average</i>	<i>Minimum</i>
<i>East</i>	52.34	13.82	-16.11
<i>South</i>	13.98	1.51	-6.40
<i>West</i>	68.65	58.57	52.51
<i>Top</i>	3.96	0.09	-6.05

4.3 ACCURACY IMPROVEMENT

As a way to improve the interpolation accuracy over the initial test, the number of samples in the pressure database is increased by using the employed

approximation technique (Section 3.3.1). To gain confidence in prediction accuracy, more prediction tests are conducted.

4.3.1 INCREASE THE NUMBER OF SAMPLES

The database with a higher number of samples is tested, now using 21, 41, and 81 samples. Newly added samples of urban contexts are generated randomly and with equal probability for all samples in the database, in the same way as for the initial test (Section 4.1).

The total computation times in generating the surface pressure data are observed, Table 9, regarding the assessment of new sample cases with CFD simulations. However, these computation burdens do not noticeably increase the run-time for the users. Errors were observed on the west surface, one of the most problematic surfaces in the initial test, and errors were observed on the south surface that showed in the acceptable range.

Table 9 Computational time with number of samples (hours)

<i>Number of samples</i>	<i>11</i>	<i>21</i>	<i>41</i>	<i>81</i>
<i>Total Simulation time (hours)</i>	3.89	5.2	9.9	26.88

As a result, the accuracy of the numerical search model has been gradually improved on the west surface, with the increase in the number of samples, Figure 17. The test with 41 samples showed a significant improvement, with a reasonable

average error of 19.93% as shown at Table 10. However, an accuracy increase in the 81 case test is not very significant compared to 41 sample cases, but the computational time for assessing 81 samples was higher by 17 hours.

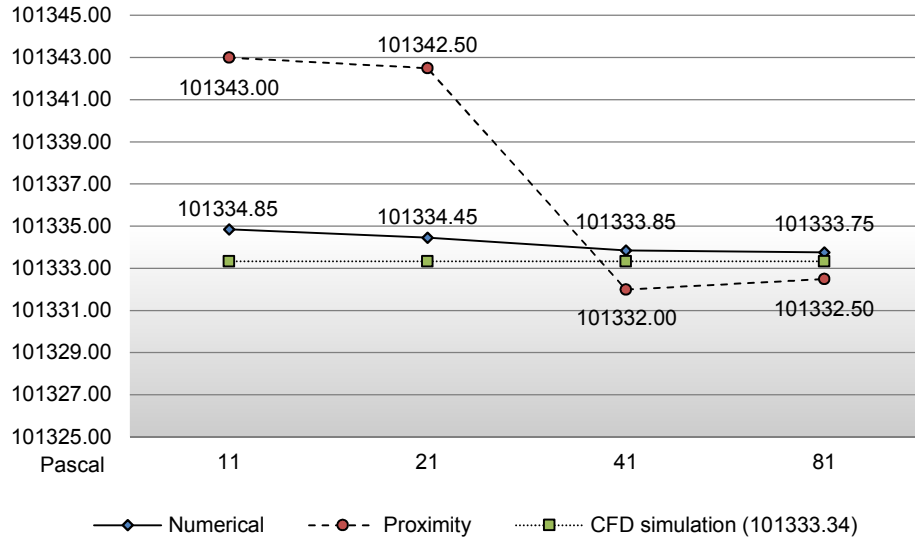


Figure 17 Accuracy increase with more samples on west surface (Pascal)

Table 10 Average error with more samples on west surface (%)

Number of samples	11	21	41	81
<i>Numerical</i>	58.57	43.18	19.93	16.06
<i>Proximity</i>	374.39	335.65	-51.76	-32.39

Apart from the accuracy, different characteristics of the two approximation techniques are shown: numerical and proximity search. In the proximity search, under-predictions were found with 41 (and 81) samples, even if over-predictions were found with the smaller number of sample. This means that the search model found a new sample that was not part of the 11-sample case. This new sample is

geometrically more similar to the new urban context input. Its associated pressure data, which happens to be lower than, but closer to the benchmark solution, was acquired as an output. In contrast, the numerical search consistently over-predicted with smaller error ranges for increasing numbers of sample.

The proximity search method with 81 samples showed 32.38% error. This is very close to the limit of acceptable range. However, the 21 and 11-sample cases proved unreliable with more than 300% error. The 41-sample case showed an unreliable result with 51% error, but this is a significant improvement over the 11-sample case; its computational cost is 36.83% better than the 81-sample case.

Figure 18 shows the prediction result on the south surface and indicates that the overall accuracies are improved by both the numerical and the proximity model, even if the numerical model shows a slight decrease. However, overall accuracy with any number of samples by both models stays reasonable with 9~13% error, at Table 11.

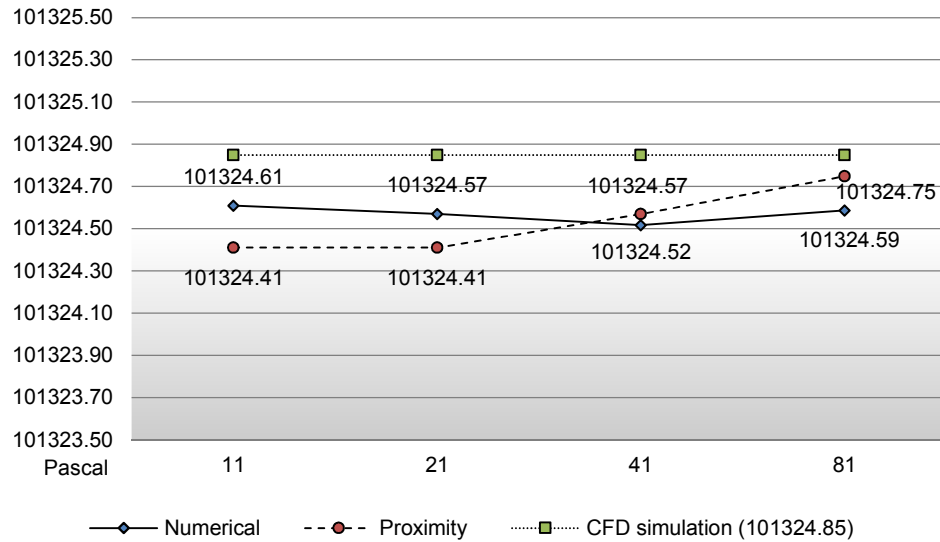


Figure 18 Accuracy increase by more samples on south surface (Pascal)

Table 11 Average error with more samples on south surface (%)

<i>Number of samples</i>	<i>11</i>	<i>21</i>	<i>41</i>	<i>81</i>
<i>Numerical</i>	-9.27	-10.76	-12.86	-10.14
<i>Proximity</i>	-16.97	-16.97	-10.82	-3.84

The proximity search provided a better solution than the numerical 41 and 81-sample tests. Samples in these two cases have a geometrical resemblance, being closer to the input, along with its associated pressure data. The 11 and 21-sample tests showed identical results, meaning that the same case is used in both, since the method could not find another sample with better geometrical resemblance.

In this section, the number of samples in the database was increased for prediction accuracies. They were tested with two interpolation models: the numerical search as the primary for high accuracies, and the proximity search as the secondary to

ensure finding a solution. The 41-sample test showed reasonable accuracies overall for its computational time, while showing good accuracies on the most problematic surfaces in the initial test.

4.3.2 ACCURACY TEST FOR NEIGHBORHOOD VOLUME

After the accuracy goals are met in Section 4.2, more test cases are conducted to gain confidence in accuracy for other geometrical conditions, particularly neighborhood volume. Accuracy is observed with changes in varying parameters - length and height - while keeping the other parameters constant, such as 5 m/s westward wind speed and flat topography. The west surface is the focus because it is in windward conditions where the highest ranges of errors generally occur, as demonstrated in the previous model tests (Section 4.3.1).

4.3.2.1 VARYING LENGTH

Three (3) lengths of neighborhood are tested: 100, 200, and 400m. The height of the neighborhood is constant at 15m. As a result, pressure maps on the west surface are examined with CFD simulation, Figure 19. Most notably, the hierarchy of pressure intensity is in good agreement for any length, showing higher pressures on lower areas, indicated by arrows.

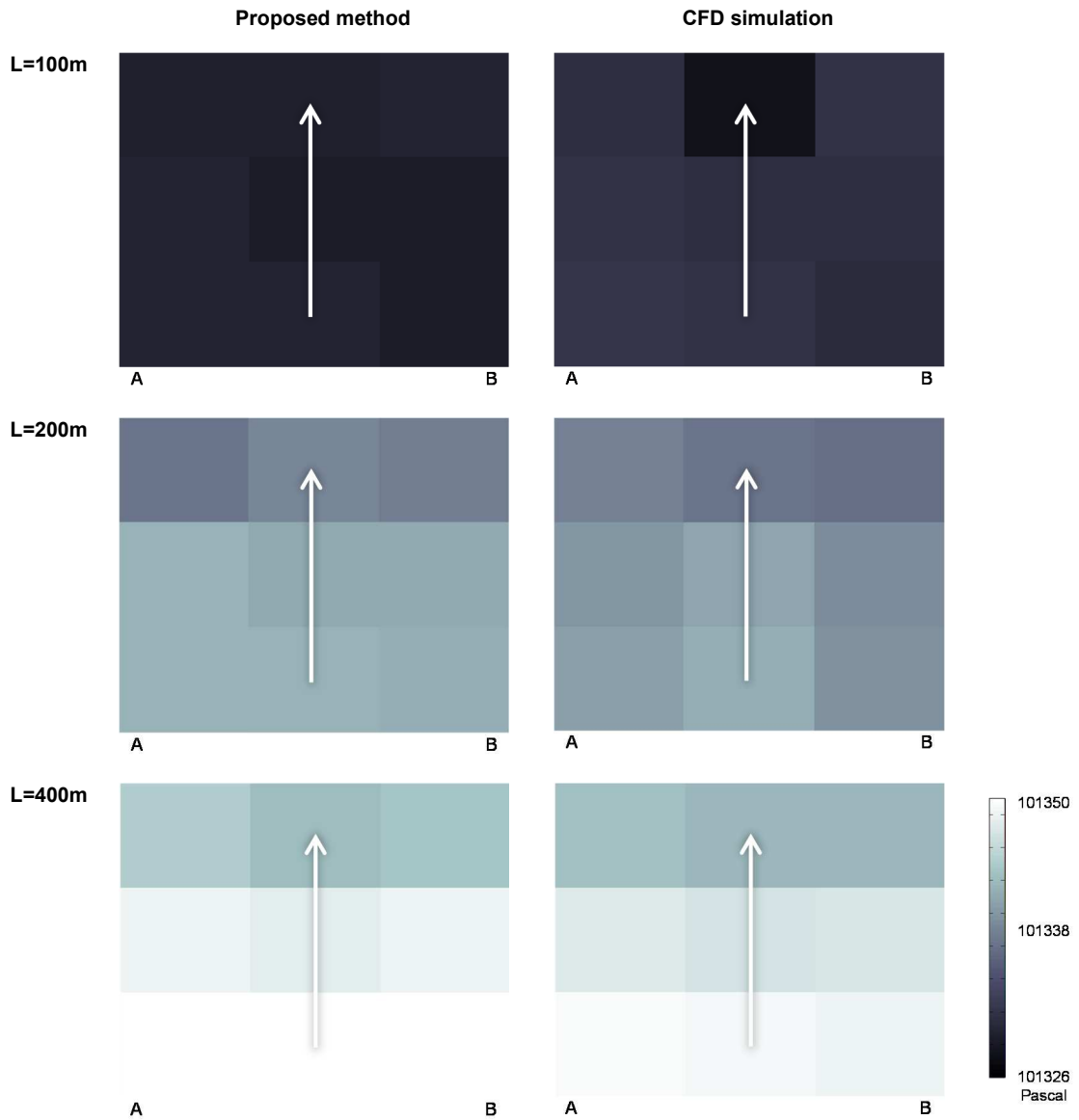


Figure 19 Predicted pressure on west surface with different neighborhood lengths (Pascal)

Table 12 shows the normalized error. Average errors for any length are within the good range, 0.54% up to 2.34%. Maximum and minimum errors in 200m and 400m cases are reasonable below 20%. Over 20% errors were found for 100 m case, which yet is closer to the standard for reasonable errors than to the standard for

unreliability. Hence, the model’s accuracy is demonstrated acceptable for all tested neighborhood lengths.

Table 12 Normalized errors for west surface with different neighborhood lengths (%)

<i>Length in 100m</i>			<i>Length in 200m</i>			<i>Length in 400m</i>		
<i>Maximum</i>	<i>Average</i>	<i>Minimum</i>	<i>Maximum</i>	<i>Average</i>	<i>Minimum</i>	<i>Maximum</i>	<i>Average</i>	<i>Minimum</i>
28.84	0.54	-22.06	9.34	2.34	-14.88	5.78	0.67	-10.63

4.3.2.2 TESTING VARYING HEIGHT

Three (3) different heights of neighborhood are tested: 15, 30, and 60 m. The neighborhood length is constant in 400 m. As a result, pressure outcome on the west wall is examined with the benchmark solution for each case, Figure 20. The hierarchy of intensity is in good agreement, similar to the observations found in testing different lengths (Section 4.3.2.1). However, the 60 m high case shows a noticeably higher range of errors, potentially because of the lack of similar samples to match the tested case.

Table 13 shows the normalized errors for the different heights. Average errors are in either good or reasonable range for any height, 2.8% up to 7.98%, even though the error rate increases for the taller neighborhoods. Maximum and minimum errors on 30 m and 60 m cases are shown to be reasonable. More than 20% errors occurred for the 15 m case, but this is still within the reliable range.

In summary, the test cases demonstrated that the proposed model has acceptable accuracy for the volumes of neighborhoods with different heights and lengths.

Therefore, within the range of the parameters, confidence has been gained for the model's accuracy.

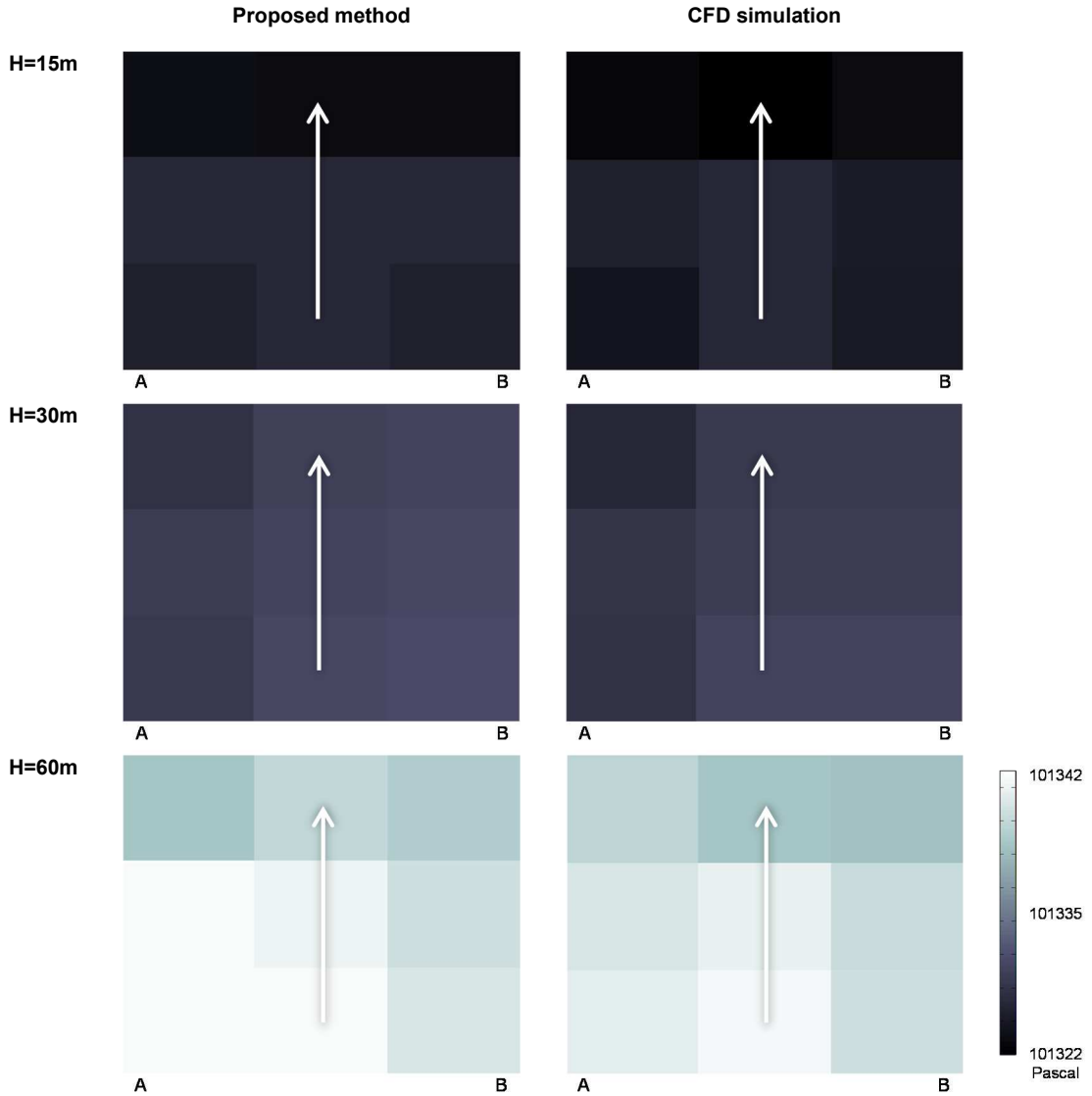


Figure 20 Predicted pressure on west surface with different neighborhood heights (Pascal)

Table 13 Normalized errors on west surface with different neighborhood heights (%)

<i>Height in 15 m</i>			<i>Height in 30 m</i>			<i>Height in 60 m</i>		
<i>Maximum</i>	<i>Average</i>	<i>Minimum</i>	<i>Maximum</i>	<i>Average</i>	<i>Minimum</i>	<i>Maximum</i>	<i>Average</i>	<i>Minimum</i>
25.06	0.28	-26.94	7.95	1.20	-14.88	19.95	7.98	-1.05

4.3.3 SENSITIVITY TEST FOR TOPOGRAPHIC CONDITIONS

With confidence in prediction accuracy (Section 4.3.2), the sensitivity of the proposed method is tested to examine how well it conforms to existing empirical studies of how topographic configurations affect local wind speed. Four (4) different site geometries, Figure 21, are generated and tested, including valley, hill, flat, and mixed. The neighborhood is in the same volume for all test cases, Table 14, focusing on the changes in topographic impact. Wind speed of 5 m/s progresses from the west so that the west surface of the neighborhood is the windward and the east surface is the leeward.

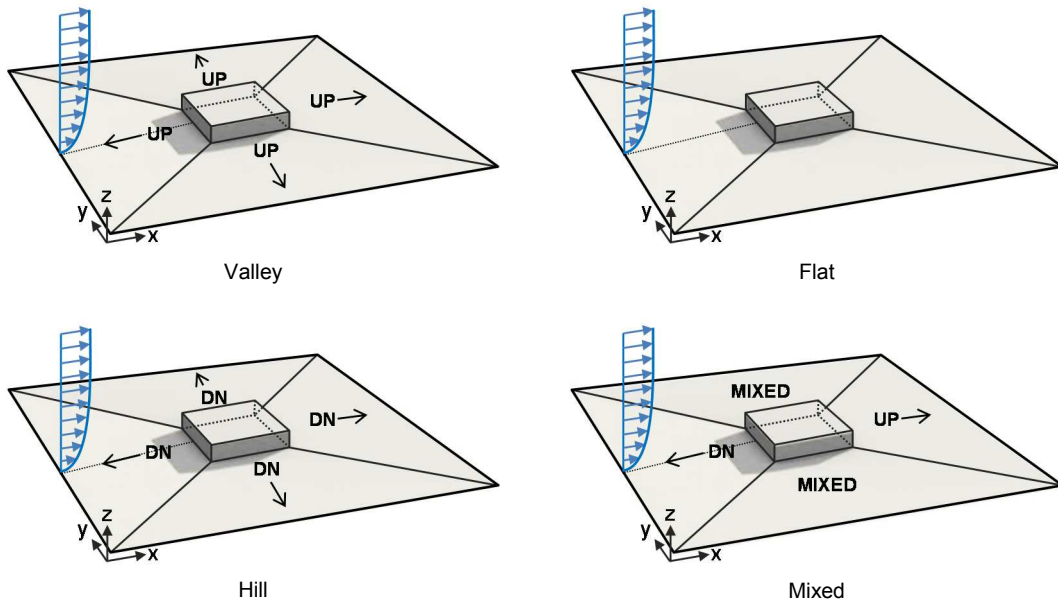


Figure 21 Four site geometries for prediction test

Table 14 Parameters for four site geometries

	Neighborhood length (m)	Neighborhood height (m)	West slope	East slope	Wind speed (m/s)
Valley	200	30	1/10	1/10	5
Flat	200	30	0	0	5
Hill	200	30	-1/10	-1/10	5
Mixed	200	30	-1/10	1/10	5

As a result, Figure 22 shows the predicted pressure on the west surface for the tested site geometries. The hill case shows higher pressure than the flat one; however, the flat one is higher than the valley case. The mixed case shows even higher pressure than the hill case, because of its overall geometric configuration with the direction of wind, conforming with existing empirical studies (Sierputowski, Ostrowski, and Cenedese 1995, Ferreira et al. 1995).

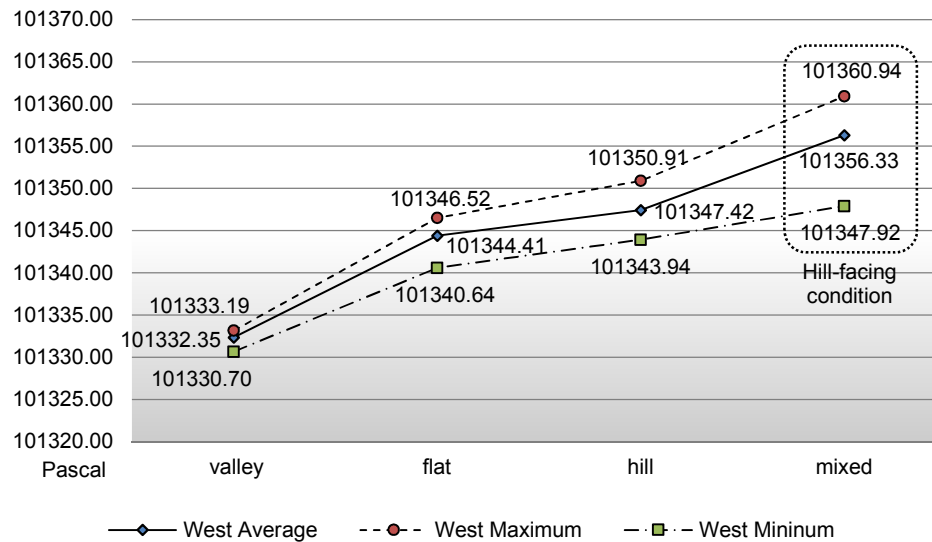


Figure 22 Predicted pressure on west surface for four site geometries (Pascal)

The mixed case also showed a higher range of pressure by 40%, compared to the average range over the other three cases. More interestingly, it is even higher than the hill by 8.9 Pascal. This is because eastward wind is forced to progress through the smaller volume of atmosphere above the west and east slopes sequentially; thus higher wind speed occurred to increase surface wind pressure. This demonstrates the significant influence of the geometric configuration of the entire site on local wind conditions.

The predicted pressures on the east surface are shown in Figure 23 for impact of different site geometries. Similarly, for the west surface, the hill case shows higher overall pressure than the two other cases, the valley, and the flat. However, for the mixed condition, the pressure outcome shows as low as the valley, because of their geometrical similarity in part on the slope on the west of the neighborhood. This shows the primary influence of immediate slope.

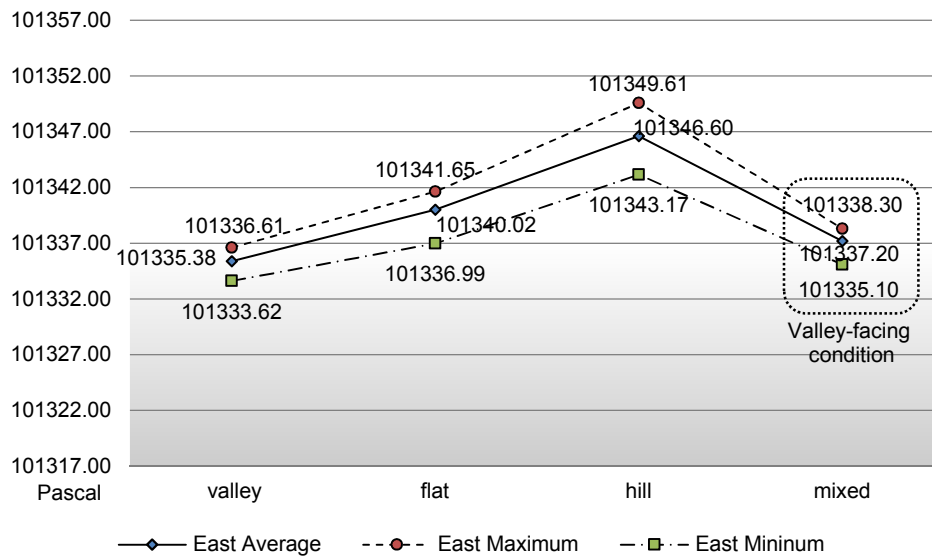


Figure 23 Predicted pressure on east surface for four site geometries (Pascal)

For the south surface, the predicted pressure is shown, Figure 24. In the valley, flat, and hill cases, the pressure results show the same hierarchy compared to the west and east surface, confirming the influence of the surrounding slopes. The mixed type result is between the hill and flat type, since the topographic geometry of mixed type has the character of both types, transitioning from one to another.

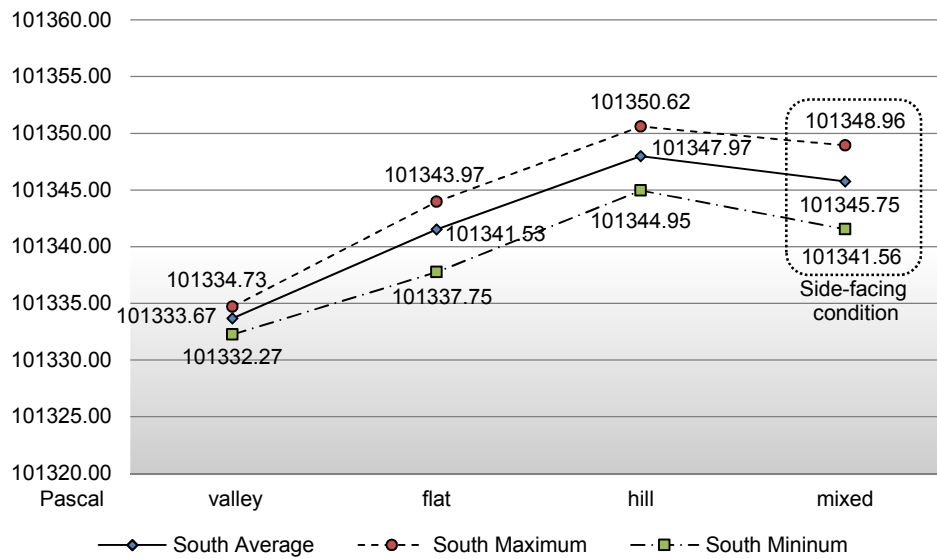


Figure 24 Predicted pressure on south surface for different site geometries (Pascal)

This section observed the influence of topographic conditions on surface pressure of neighborhood boundaries. Because the hill case figuration allowed more available free stream wind, it showed the highest overall pressure. However, the mixed case showed even higher pressure, locally on its windward west surface, showing the importance of the entire site geometry. This also conforms to existing empirical studies on topographic impact on local wind condition. Therefore, the model's sensitivity has been demonstrated successfully, achieving one of the objectives.

4.4 SUMMARY

The current chapter developed the pressure database to emulate the capacities of CFD to predict wind pressure with the proposed interpolation method. After the partial accuracy failure in the initial database with 11 samples, the number of sample geometries was increased for reducing the ranges of errors. With 41 samples, reasonable accuracies were achieved toward the prediction goals, with below 15% error for most test cases. At the same time, a reasonable computational time (10 hours) was spent in CFD simulation of all site samples for the database.

With more case studies, confidence in prediction accuracies was gained for the different volumes of the neighborhood. For any length and height, the average errors were in the good or reasonable range of below 10%, while the maximum and minimum errors were in the reliable or close to the reasonable range of 20%.

The method also showed high sensitivities for geometric variables, while confirming existing and empirical studies. This is one of the objectives of the dissertation stated in Section 1.3, supporting incremental studies in early stages of building or neighborhood design processes, as the advantages over more efficiently than the empirical models or building-averaged models.

For future considerations, more samples of neighborhood sizes can be added for skyscrapers-dominant conditions, such as New York City or Chicago. Samples for steeper slopes can be also added for very hilly cities such as San Francisco that has 1/5 and higher slopes covering more than 10% of its area.

CHAPTER 5 SPEED DATABASE DEVELOPMENT

With the proposed model and its employed techniques, the speed database is developed, accounting for a large urban area, up to a few kilometers. Topographic effect is integrated by conducting virtual wind tunnel tests with CFD simulation. To enhance data portability, wind reduction ratios are developed for terrain and slope that affect local wind speeds. To save computational resources, a single instance of an urban condition is geometrically modeled for each terrain type on a slope. A relationship between pressure and speed is also defined based on an existing model that is typically used in building-scale studies.

5.1 GEOMETRIC CONDITIONS

5.1.1 TERRAIN

Terrains are geometrically constructed with buildings and streets on a 1000 m by 1000 m site, Figure 25. They are based on the boundary layer parameters (Table 2) from “Airflow Around Buildings,” a chapter from the handbook of the American Society of Heating, Refrigerating, and Air-Conditioning Engineers (ASHRAE).

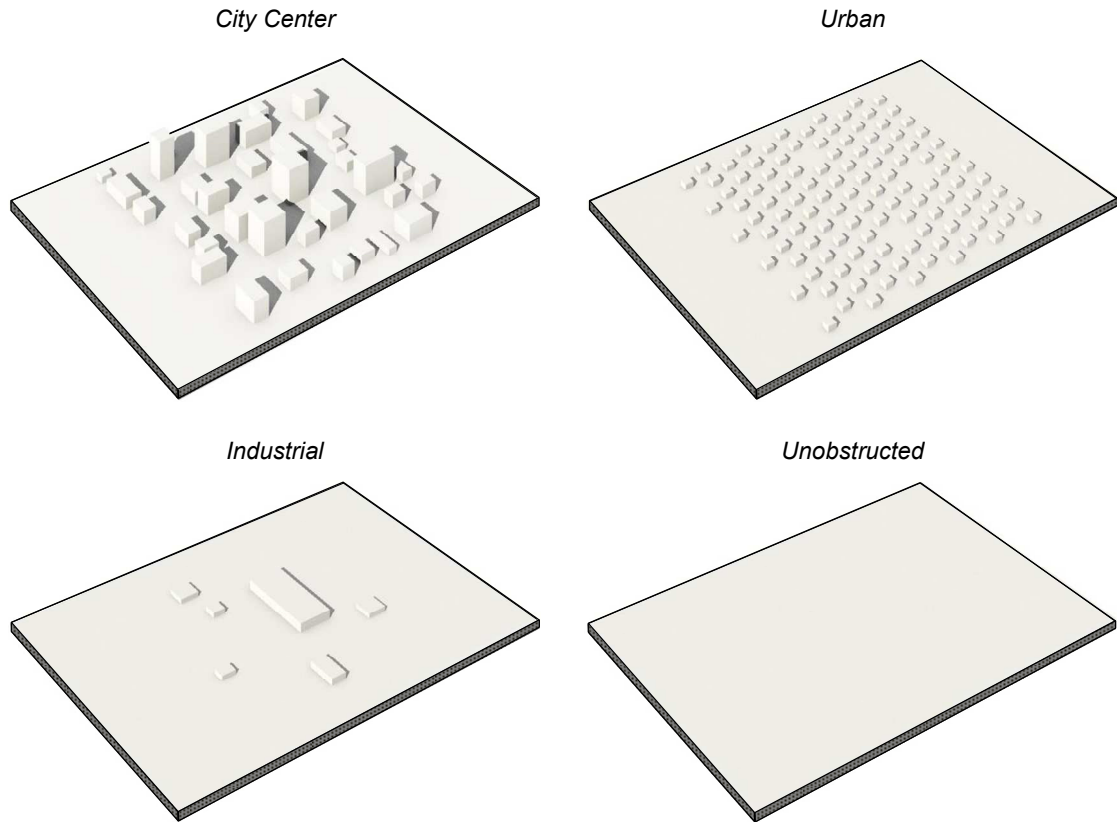


Figure 25 Geometrical input of each terrain type for CFD simulations

Buildings are in orthogonal shapes and windows are omitted for simplification. The dimensions of streets are based on typical U.S. streets (Daley 2007, Steiner and Butler 2006): 15 m for major two-way streets and 9 m for the minors. Streets are composed with 3 m wide roadways for vehicles and 2 m wide sidewalks for pedestrians. Trees in streets are not included for avoiding complexities and their high computational intensity in CFD simulations. For surface materials, generic properties of concrete and asphalt are chosen for buildings and streets, respectively, based on ASHRAE Materials References (ASHRAE 1993).

5.1.2 SLOPE

To integrate the impact of topographies on urban conditions, a slope is added in the terrain geometries for CFD simulations, Figure 26. While keeping the exposed surface areas of buildings within a terrain type, negative and positive slopes are increasingly applied every 1/20, up to the predefined ranges from the database algorithm, for typical urban areas in U.S. (Table 4). Positive slope means that the ground tilts up from the local site where outgoing wind is measured, being equivalent to a valley.

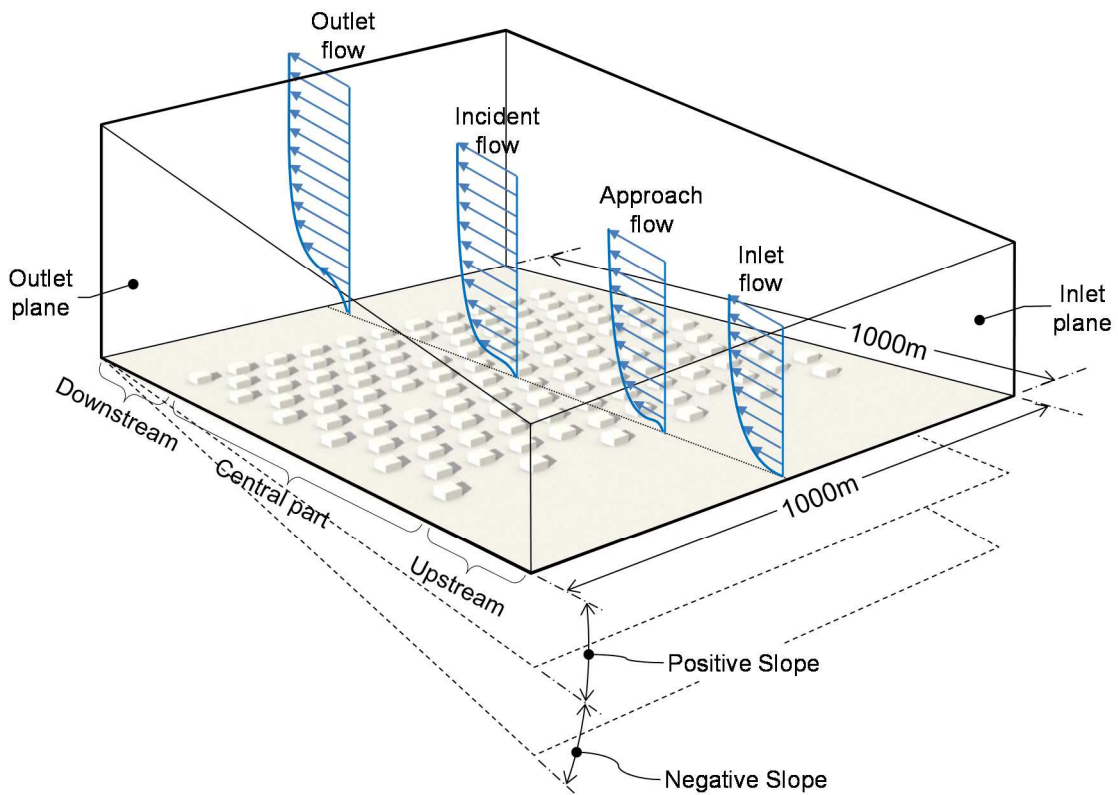


Figure 26 Slope, added to the terrain geometry for CFD simulations

5.2 WIND SPEED ASSESSMENT

With the geometries of terrain and topography, CFD is used to assess the wind speed. Measurement locations are at the outlet and the inlet for the local and the regional, respectively. For measuring outdoor wind speed, the CFD settings are borrowed from the pressure database (Section 3.1.3), which lists the recommended applications of the computational domain sizes, the turbulence model, and meshing. ANSYS FLUENT 14 was used for CFD simulations as used in developing the pressure database (Chapter 4)

The CFD simulation results are presented at Table 15 and Table 16, showing wind speeds and pressure gradients on a cross-sectional plane in the middle of each domain. Most notably, slopes played a significant role, across all terrain types, in that negative slopes induced higher local wind speeds near outlet planes, compared to positive slopes. It is because wind progresses toward the smaller volume of atmosphere, where pressure becomes lower as shown in the pressure gradients. The impact of slopes is more evident with fewer buildings, showing buildings' roles as obstructions within each terrain in effectively reducing wind speeds.

Table 15 Wind patterns by terrains on slopes – city center and urban

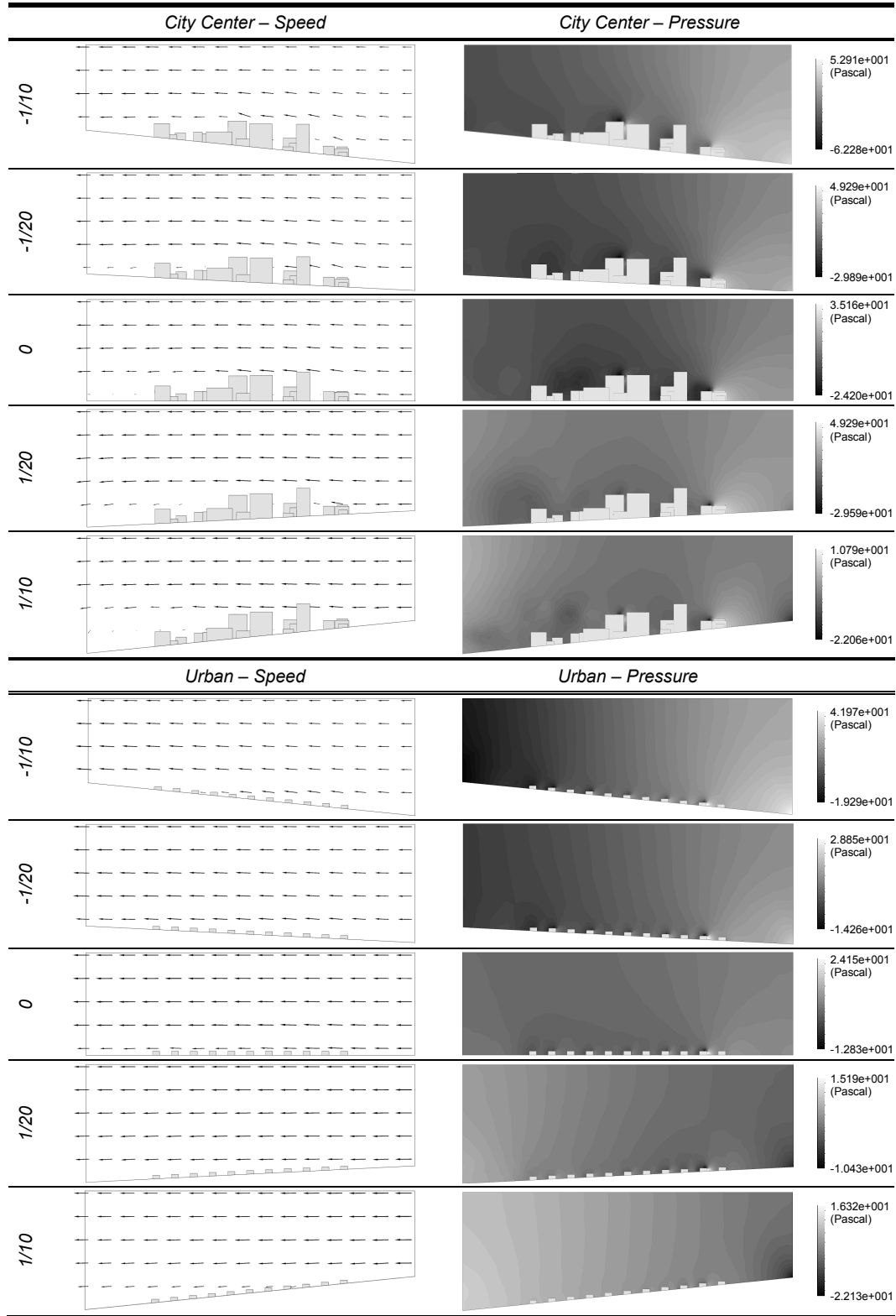
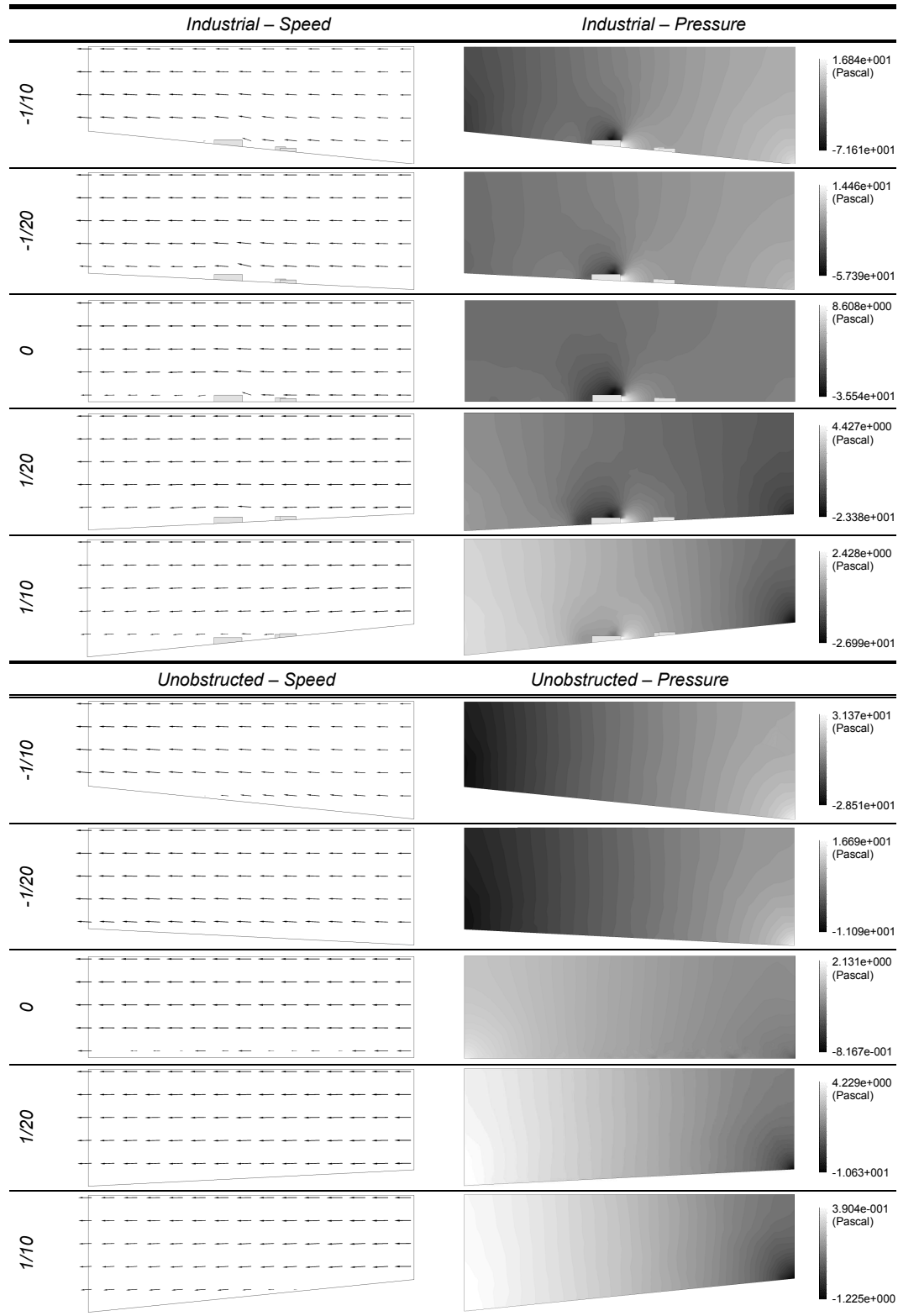


Table 16 Wind patterns by terrains on slopes – industrial and unobstructed



On the other hand, the volume of buildings effectively intensifies the ranges of pressures. This is because higher differences are shown around large buildings, regardless of terrain types. Thus, it is not surprising that the city center terrain has the highest ranges by 115.19 Pascal; nearly twice as high as the urban terrain for the same -1/10 slope. Similarly, the industrial terrain has a higher range than the urban terrain by 21.19 Pascal, because it larger buildings even if only few exist (Figure 25), compared to any building in the urban terrain. Therefore, resultant wind assessments of each terrain on various slopes are reasonable, based on the wind pattern analyses.

5.3 WIND REDUCTION RATIOS

To enhance data portability with the CFD simulation results, wind reduction ratios are developed for the localized wind speed at outlet planes over the regional wind speed at inlet planes. Wind speeds are averaged across the site at 10 m above ground, which is usually the same height of anemometers to record regional wind speed for TMY weather data (Wilcox and Marion 2008, ASHRAE 2009).

The reduction ratios are normalized by the flat slope case that is assumed in the existing mathematical method (Section 2.2.3). This means the lower the ratio is below 1, the less wind reduction occurs, due to the positive slopes under the same terrain type. The higher the ratio above 1, the more wind reduction occurs for the negative slopes.

The resultant wind reduction ratios are shown at Figure 27, for sloped terrains. The terrains with more obstructions have the smaller impact in general, because buildings interfere with wind flows regardless of added slopes at the measurement height. This trend agrees with the wind pattern analyses with the CFD simulation results in Section 5.2.

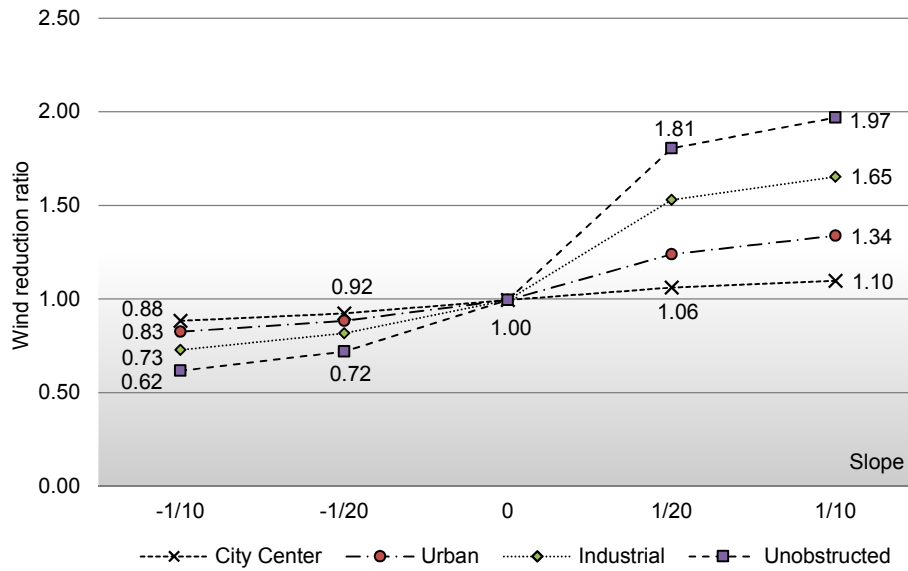


Figure 27 Wind reduction ratio for sloped terrain, normalized by flat terrain

The city terrain, in particular, has the least impact on changes in wind reduction ratio, since it is composed with the densely populated tall buildings with larger footprints, compared to the other terrains. As a result, the city terrain reduces more by 1.10 times due to 1/10 slopes, while the unobstructed terrain reduces more by 1.97 times for the same topography. This result justifies the integrating of buildings into the proposed method.

In accordance with the CFD results, positive slopes in the urban terrain reduce wind speeds more effectively than with negative slopes. This tendency applies to all terrain types with varying intensity. The average ratio over all terrain types shows that the 1/10 slope reduces more by 1.51 times than flat slope; while -1/10 slope reduces less by 0.76 times.

With increments in slopes, topographic effects on changes in wind reduction ratio become smaller, for both negative and positive slopes. The unobstructed terrain, for an example, showed the ratio increase by 81% (from 1 to 1.81) by adding a 1/20 slope, but it is only 10% increase (from 1.81 to 1.97) by adding another 1/20 slope. This trend holds true for all terrain types with varying degrees. This means that there are growth limits for the ratio changes in wind speed reduction if steepness increases.

5.4 SUMMARY

The current chapter developed the speed database with the terrain definition in the existing mathematical method with the added slope. Through CFD simulations of geometry samples, the topographic effects are embedded in the database. The reduction factors were developed for data portability, which also facilitates the calibration process. The accuracy of the speed database will be evaluated in the model test in the following chapter, as the part of the primary outcome.

CHAPTER 6 MODEL EVALUATION

The current chapter evaluates the proposed model for accuracy and computation efficiency, with the pressure database and the speed database that were developed in Chapter 4 and 5. The interpolation method in Section 3.3 is used to predict surface wind pressure on a neighborhood's volumetric boundary, Figure 28. The result is compared with a benchmark solution by the full-scale CFD simulation for the same urban geometries and materials.

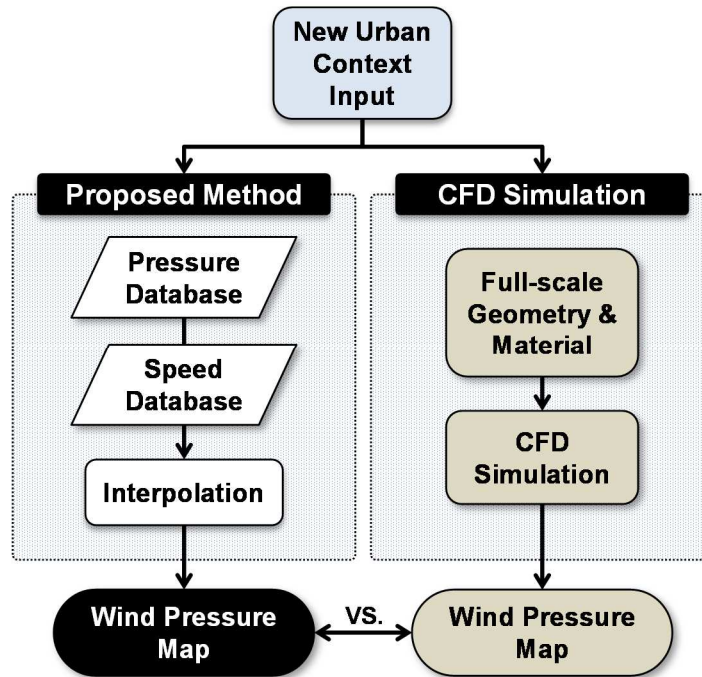


Figure 28 Model test with the CFD simulation

6.1 TEST CONDITION

The test condition has a neighborhood volume of 50 meters in height and 200 meters in length, and it sits on a mixed slope with the negative slope on the west and positive slope on the east, Table 17. Wind in 3.4 m/s comes from the west, which is the same speed and direction for the prepared pressure database (Chapter 4). All surrounding slopes have the urban terrain, which is geometrically shown with the slope and neighborhood volume at Figure 29.

Table 17 Parameters for the test condition

<i>Neighborhood length (m)</i>	<i>Neighborhood height (m)</i>	<i>West slope</i>	<i>East slope</i>	<i>Wind Speed (m)</i>	<i>Terrain type</i>
200	50	-1/20	1/10	3.4	Urban

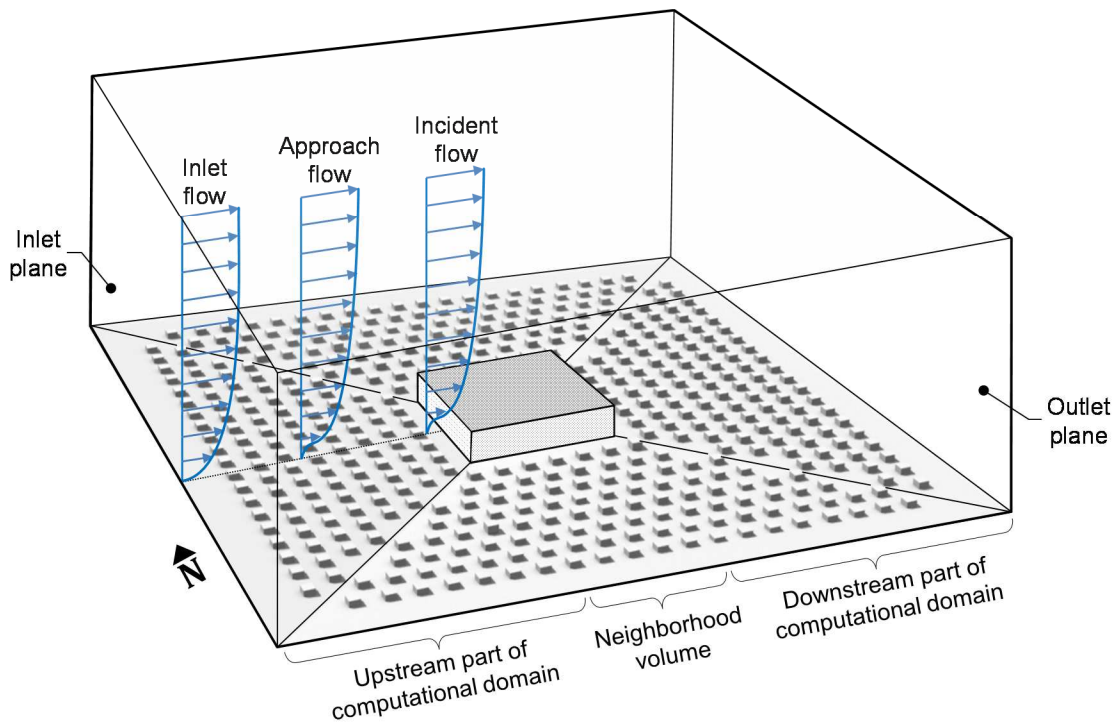


Figure 29 Urban terrain on the test condition

6.2 RESULT ANALYSIS

To analyze the resultant pressure by the proposed model, two comparisons are made, first with no-terrain, and second with the terrain, both of which have the same test conditions for the slope and neighborhood volume (Table 17) in the full scale CFD simulation. The first comparison allows understanding of the impact of terrain integration, while the accuracy and computational efficiency are fully analyzed in the second comparison.

6.2.1 COMPARISON WITH NO-TERRAIN

The pressure maps at Figure 30 show the hierarchy of pressure intensity on individual surfaces. The first set in the left column is predicted by the proposed model, with the no-terrain solution by CFD simulation being on the right column.

By reviewing each surfaces, the most significant differences are found on the west surface, which is in the windward condition by the test setting, facing directly against the eastward wind. The vertical direction of pressure hierarchy is flipped compared to no-terrain condition, while overall intensity across the surface is reduced. This is due to the buildings and streets in the terrain that reduced the wind speed and pressure, which happens more at the bottom than the upper area.

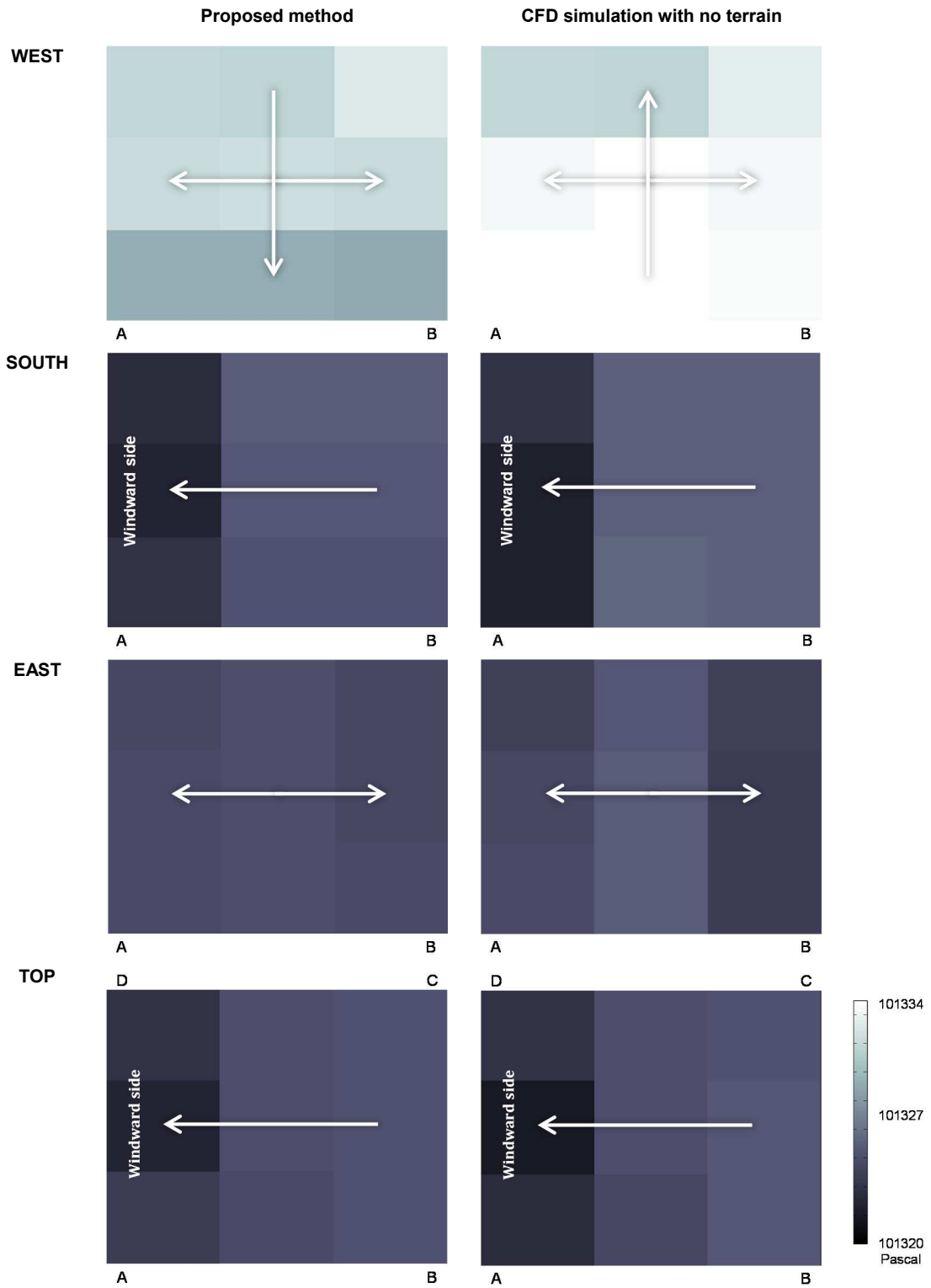


Figure 30 Pressure outcome, compared with no-terrain solution (Pascal)

On the south and the top surface, the hierarchy is mainly governed by the proximities to the windward surface; the nearer to the west surface, the lower the pressure. On the windward side of the south surface, the proposed method shows a higher pressure on the bottom than the upper area, which is different to the no-terrain solution, showing the influence of the terrain integration. This influence is also shown by the proposed method on the east surface with visibly lower overall pressure, even though the hierarchies for both cases are nearly identical.

The prediction errors are analyzed at Table 18. Most noticeably, the maximum error on the west surface is in the unreliable range with 42.03%, which is the worst in any prediction test other than the initial one with 11 samples. The top surface has even lower accuracies than the initial prediction (Table 8) by 2.6% and 14.28% more in average and minimum errors. Hence, the prediction accuracy is unreliable, and so is the hierarchy of pressure intensity result, due to the absence of terrain in the CFD simulated solution. This again demonstrates its significance of the proposed model.

Table 18 Prediction errors for the no-terrain condition (%)

	<i>Maximum error</i>	<i>Average error</i>	<i>Minimum error</i>
<i>East</i>	10.65	-1.96	-10.07
<i>South</i>	9.62	0.56	-18.00
<i>West</i>	42.03	18.88	0.31
<i>Top</i>	6.29	-2.51	-20.33

6.2.2 COMPARISON WITH TERRAIN

The pressure maps created by the proposed model are compared with the benchmark solution by CFD simulation, Figure 31. In CFD simulation, terrain is integrated to slopes. Most noticeably, the intensity hierarchies on all individual surfaces are in good agreement, horizontally and vertically. This is evident by reading white arrows on each map, starting from the highest pressure to lowest pressure. On the west surface in particular, the vertical hierarchy is corrected, which was one of the problems in comparing with the no-terrain solution (Figure 30). Another correction to the vertical direction was made on the south surface at the windward side. This demonstrates the effective terrain integration by using the interpolation method with the speed database.

On the south and the top surface, the pressure intensity is governed by the proximity to the west surface, similar to no-terrain solution, yet agreeing with the benchmark solution with the terrain. This is because the highest pressure on the windward surface has the primary impact on the other adjacent surfaces. Additionally, the pressure hierarchy on the south surface is improved in the vertical direction, compared to the initial test (Figure 15). Hence, one of the prediction goals, the hierarchy of pressure intensity within individual surfaces, has been achieved, with added considerations for terrain integration.

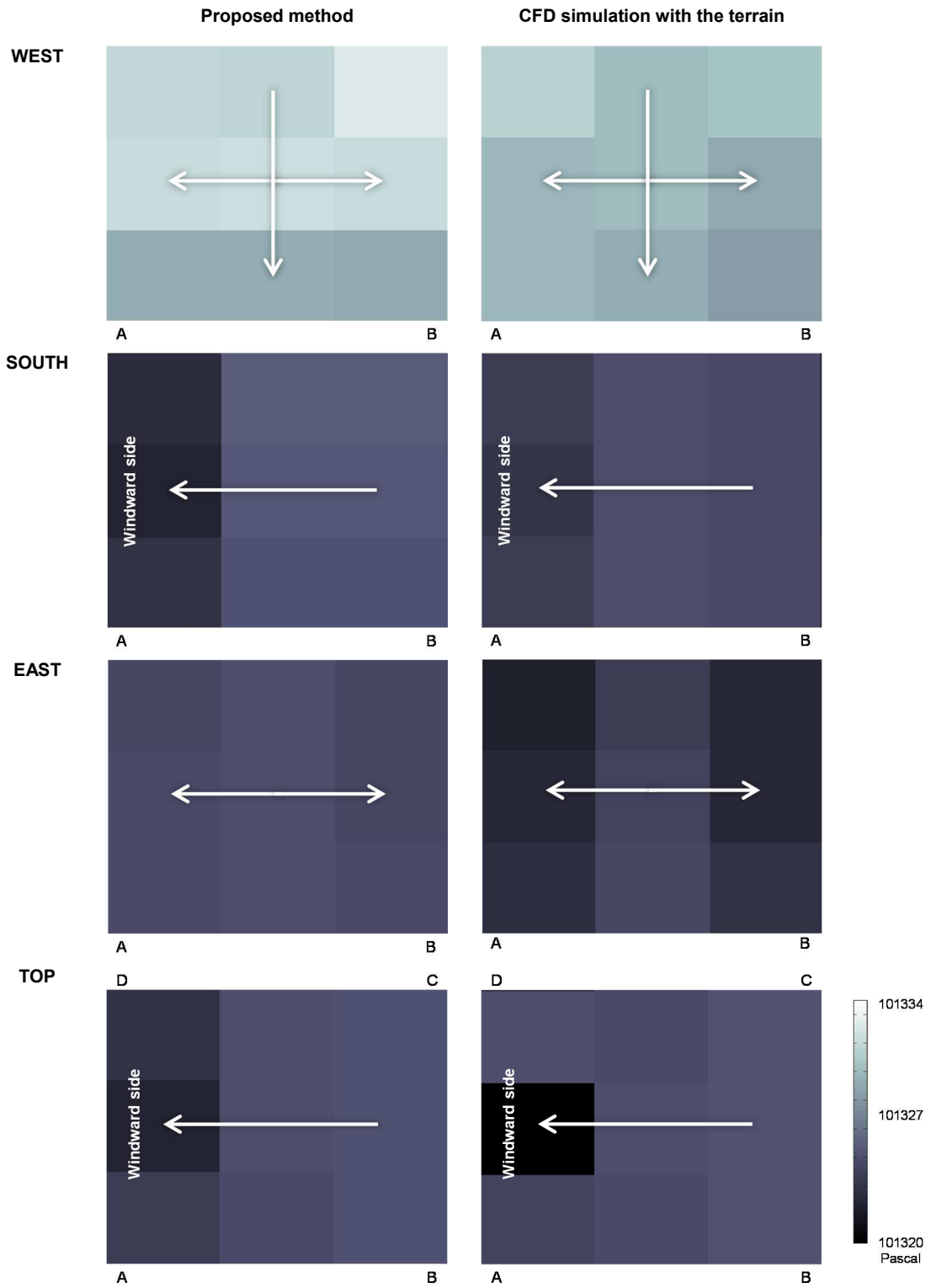


Figure 31 Pressure outcome, compared with the terrain-integrated solution (Pascal)

For the pressure hierarchy among surfaces, pressure outcome at each point of the surfaces is plotted at Figure 32. The highest average pressure is found on the west surface, both by the proposed method and the CFD simulation, due to its windward condition facing against the wind flow. The south surface has the second highest pressure, yet significantly less than the highest by 6.66 Pascal, while slightly higher than other two surfaces - east and top - by 1.70 and 0.25 Pascal.

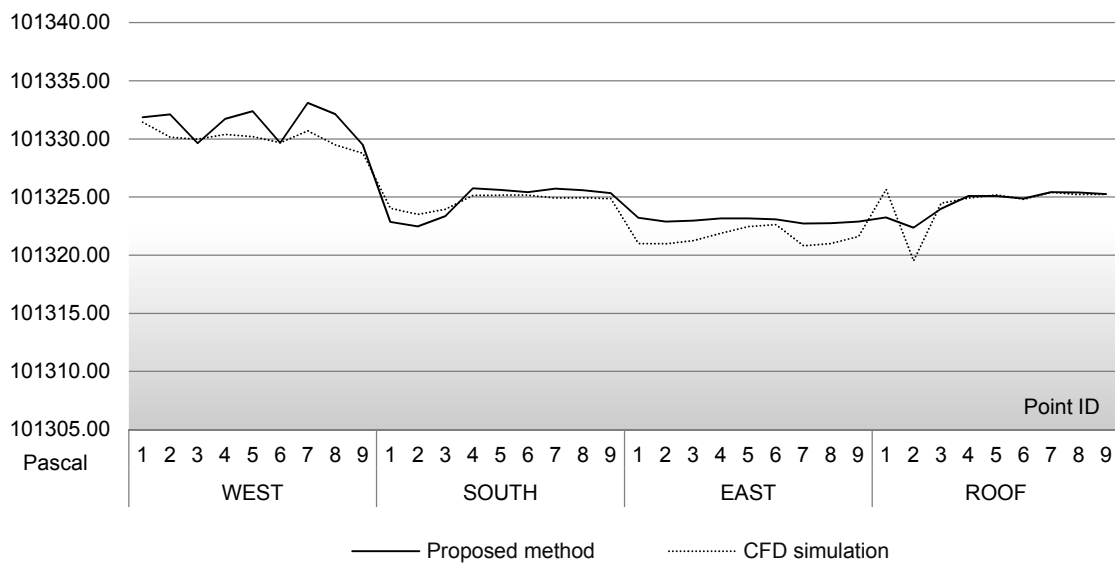


Figure 32 Pressure outcome at each point of the surfaces (Pascal)

More importantly, a discrepancy in the pressure hierarchy is absent, regarding the east surface, which required accuracy improvement in developing the pressure database (Chapter 4). The third highest average pressure intensity is on the east surface, which is in accordance with the CFD-simulated solution. This improvement is due to the reduced error by 1.99 Pascal on the lower portion of the surface (point ID of 1, 4, or 7 in the figure), proving the effectiveness of adding

samples in the database (Section 4.3). This achieves the goal of predicting the pressure hierarchy among surfaces.

The prediction errors are analyzed at Table 19. The highest average error was found on the east surface, for its problematic leeward condition. However, its maximum and minimum error is within the reasonable range, less than 20%. This is a significant improvement over the interpolation test (Table 8), which showed more than 50% maximum error.

Table 19 Prediction errors for the terrain-integrated solution (%)

	<i>Maximum error</i>	<i>Average error</i>	<i>Minimum error</i>
<i>East</i>	-3.46	-11.24	-17.00
<i>South</i>	9.02	-0.33	-6.03
<i>West</i>	2.83	-9.60	-20.32
<i>Top</i>	18.54	-0.23	-21.81

On the west surface, another problematic area due to its windward condition, the average error is significantly reduced by -50.84% on average, compared to the no-terrain condition (Table 18). In comparison to the interpolation test in the pressure database development (Table 8), errors are noticeably reduced, from 68.65% to 2.83% in maximum and from 52% to 20.32% in minimum. The accuracy on the most problematic surface has changed to reasonable from unreliable, proving that the proposed model has the intended effect.

On the top surface, increased errors are found compared to the interpolation test, from 3.96% to 18.54% in maximum, -6.05% to 21.81% in minimum. Yet, they are

still in the good and reliable range, while the average error is in the good range by 0.23%. The errors on the south surface are reasonable with less than 10% in maximum, which is 35.47% more accurate than the interpolation test. With other result analyses, the model has demonstrated its accuracy, by successfully meeting the targeted range of errors with all parameters of interest: terrain, slope and neighborhood volume.

6.2.3 COMPUTATIONAL EFFICIENCY

The computational cost in time is compared to the full-scale CFD simulation, Table 20. The proposed model counted only the runtime for users, while excluding the overhead time that was spent on developing the databases. As result, the CFD simulation spent 5103.63 seconds for the convergence, while the proposed model took only 0.308 seconds, which is 16568 times faster. Compared to the targeted goal (Section 2.4), this is 5.67 times more efficient, which a yearlong prediction can be enabled to run less than 44.97 minutes for 8760 instances in a TMY data set.

Table 20 Computational time for comprehensive model prediction (seconds)

	<i>Proposed model</i>	<i>CFD simulation</i>
<i>Total simulation time (seconds)</i>	0.308	5103.63

6.3 SUMMARY

Based on the result analysis, the proposed model showed the acceptable accuracy for the defined range of errors as well as for the hierarchies of pressure intensities within a surface and among other surfaces. The targeted computational efficiency was also met in that a year-long prediction can be processed in less than an hour. This is more than twice as fast as the goal, allowing a few design options to be assessed in a day.

By comparing the pressure outcome to the full scale CFD-simulation with and without the terrain, the refinement process and overall interpolation process in Section 3.3 have proven their effectiveness with the acceptable accuracies. At the same time, it is demonstrated that the increased number of samples and their associated surface pressure data, as described in Chapter 4, are still valid because they improved accuracy, compared to the initial interpolation test. This is noticeable first because of the added consideration in the wind speed development, and second its added refinement process, both of which possibly carried their own sources of uncertainties in simplification.

CHAPTER 7 CONCLUSION

This dissertation developed an urban-conscious wind downscaling model that can rapidly assess the impact of built environments to predict surface wind pressure and local wind speed for early design stages. The main modeling goals were achieved allowing architects and urban designers, non-experts on simulations domains, to quickly assess surrounding urban conditions comprehensively with buildings and topographies for areas up to a few kilometers in diameter.

The current chapter revisits the research objectives that were guided by the literature reviews. The employed methods and techniques are highlighted with the focus on their contribution to achieve the objectives, before summarizing key results of the new model toward the prediction goals. Moreover, limitations are summarized, to suggest future studies.

7.1 RESEARCH OVERVIEW

The literature reviews began with investigating the fundamental challenges in wind downscaling, incurred by using a weather dataset that recorded in a fixed and distant location. While the identified issues, as summarized below, are interconnected, the leeward wind flow was found particularly difficult to solve due to the lack of climate data. The existing approach was introduced, but found not sufficient solutions in several situations:

1. Leeward wind flow
2. Lack of topographic effect
3. Homogeneity in surrounding terrains

To find a more feasible solution, existing downscaling methods were reviewed: canyon, outdoor nodal model, and CFD. Regardless of their individual potentials, no single use of these methods could either fully address the issues or satisfy the needs for early stage design. However, CFD was found most appropriate, mainly because of its capacities in geometrical sensitivities and topographic effect, which are crucial for assessing the urban scale of interest.

Therefore, the dissertation was led to propose a new methodological model that incorporates the capacities of CFD, while reducing its associated drawbacks in computation efficiencies and complexities. The modeling objectives, summarized below, were formulated to satisfy the needs of early stage design studies in neighborhood and building scales. Further, they make it possible to perform yearlong assessment, which is often is crucial even though time and resources are limited. The model allowed:

1. Rapid and robust assessment of surrounding urban areas
2. Pertinences for early stages in design processes
3. Geometric sensitivity for incremental design studies

While the widely accepted regional TMY data was adopted as the input, the types of output were determined not only for the neighborhood scale but also for further

uses in smaller scale studies. Hence, both surface wind pressure and local wind speed are included as the primary and the secondary output, respectively. Prediction goals were established with the ranges of acceptable errors in comparison to the full-scale CFD simulation, which is the conventional method. The model offers high computational efficiency that allows assessing a few design options in a day with limited resources.

7.2 FINDINGS AND IMPLICATIONS

7.2.1 PREDICTION GOALS

With computational efficiency as the one of the most important prediction goals, the process of creating and exploiting databases was the crucial step. Samples of existing urban contexts were geometrically generated and assessed for their associated surface wind pressure. This data is stored and retrieved so that non-experts, such as architects and urban designers, can avoid real-time runs of CFD simulations that require high computational resources and expert knowledge.

As a result, when compared to the full-scale CFD simulation (Section 6.2.2) the proposed method demonstrated its exceptional computational efficiency, 16568 times faster than the conventional method. This speed would enable a whole-year calculation with TMY's 8760 hours of data, requiring only in a few tens of minutes with a personal desktop computer.

In the model test, the accuracy goals were achieved with less than 10% errors in average and less than 20% in maximum, being lower than the defined ranges of acceptable errors, over all surfaces of the neighborhood volume. The other accuracy goals, which are important for the further uses of model in smaller scale studies, were also achieved: hierarchy of pressure intensity on individual surfaces and among other surfaces.

7.2.2 MODELING OBJECTIVES

The model's robustness was achieved in three levels, other than its demonstrated accuracy. First, by the use of CFD, the topographic effect was embedded in the database, responding to one of the challenges in the existing downscaling techniques. Second, the empirical urban boundary layer was integrated to wind speed prediction by calibrating the existing method as a part of the interpolation process, mitigating the identified weakness in using CFD. Third, diverse terrains can be studied in accordance with wind direction, responding to the identified issue with homogeneity.

The pertinence of the model was enhanced by the simple use of only a few input parameters. This is another aspect of high computational efficiency. Representing urban conditions around a site of interest, the parameters include surrounding slopes, terrain types, volume of neighborhood, and regional wind speed.

Geometrical sensitivity was accommodated in the unit topography and in the composition of a site, regarding the scale of architecture and urban design. The degree of slope in a unit topography can vary, positively and negatively up to 1/10, accounting for the urban areas of the most US cities. A site was composed with four unit topographies around a neighborhood so that the model can represent diverse urban conditions such as valley, hill, flat, and mixed.

7.3 LIMITATIONS AND FUTURE PERSPECTIVE

7.3.1 GEOMETRIC SIMPLIFICATION

A geometric simplification in the unit topography may cause inaccuracy. A single slope constitutes the unit, which however cannot represent complex multi-slope conditions. Integrating the effect of multi-slope situations to the presented downscaling ratios may be a possible solution, instead of adding more samples in the database. This may restrain the number of parameters, the order of problems in employed interpolation technique. In other words, a study can be done without assessing countless combinations of positive, negative, and flat slopes of various steepness.

In the CFD setting to assess the urban contexts in the database, the volumetric boundary of a neighborhood was assumed wall surface as if it constructs a large-size building. This setting allowed focusing on overall wind flows around the neighborhood as the scale of main interest, while the intended use of outcome was

designed for smaller scale urban studies. However, penetrating wind flow through the neighborhood boundaries was not accounted, which can be further considered by excluding the walls partially or completely.

Geometric modeling of terrains in CFD simulations, as a main part of the pressure database development, has two major and one minor limitation. The first major limitation is that only one instance of an urban condition was geometrically modeled for each terrain types. However, more instances with diverse building typologies and street layouts can be further included to reflect the heterogeneities of cities. The second major limitation comes from the types of obstructions, in that only buildings and streets are considered. Even if they play the main role in outdoor wind flows, other types of built environment can be included, such as trees, street furniture, and transit shelters. The minor limitation comes from simplifications in building walls. Windows were excluded because of their minor impact on urban-scale wind flow, compared to the buildings themselves. Although not expected to make substantial changes in simulation results, they may be considered to fine tune the prediction accuracy.

7.3.2 DEFINED RANGES OF PARAMETERS

In the database development, one limitation comes from the defined ranges of input parameters, which were used to generalize urban contexts. Only limited range was defined to cover typical urban areas in U.S. cities, so that the number of urban context samples could be reduced for computational efficiency and for

data portability. However, an area with more than 1/10 slope can be accounted, by adding samples in the database.

In the speed database development, only limited types of terrain were considered, because they were carried over from the existing method. The existing mathematical method uses the urban boundary parameters, which categorize natural and built environment into only four types. To expand their application, however, other possible types can be constructed by combining the existing terrain categories. On the other hand, for unusual conditions such as skyscraper-dominated cities, new samples may be added to the database; hence, they can expand the capacities of the adopted method.

7.3.3 FIXED NUMBER OF PRESSURE OUPUTS

Another limitation may occur due to the fixed number of pressure outputs on the neighborhood boundaries. The proposed model predicts nine (9) locations on each surface of a neighborhood, totaling forty-five (45) locations. This allows the user to read hierarchies of pressure intensities within a surface as well as among surfaces. However, the total number of locations is fixed for any size of domain, which may create higher errors in larger volumes where a pressure output shall represent the larger surface area. Therefore, future studies may include integrating an algorithm to interpolate or extrapolate the prediction results in order to create more data locations.

7.3.4 LEEWARD WIND TRANSLATION

For the identified issues in wind downscaling, the proposed model has responded to two: the lack of topographic effect and homogeneity in surrounding terrains. This was explicitly achieved through the database development with CFD simulations and its application for diverse terrain conditions around the site, depending on wind directions. While the leeward wind flow issue was not directly addressed, it can be also resolved by using the proposed model with a macro scale model introduced in Section 1.2.3.2. Accounting for the topographies up to 14 km, a macro scale model first generates a regional climate data with the TMY datasets. This data then is downscaled with the proposed model for the smaller regional scale slope and the terrain, together representing urban contexts.

Another approach may include development of new model to translate the TMY data, instead of using an existing macro model, which requires high computational costs to account the entire surface of the Earth. The translation model identifies and translates wind speed in the leeward condition to its counterpart in windward condition that progresses toward the site of interest. For this development, the site-specific wind speed can be extracted from the CFD simulation results that were used in developing the pressure database in Chapter 4. While this data accounts for the surrounding slopes and neighborhood volume, the effect of terrain can be readily integrated with the reduction ratios developed in Chapter 5, along with the proposed interpolation method in Chapter 3. The translated windward data may

increase the credibility of the climatic boundary condition that can be used in the proposed downscaling model for the neighborhood scales.

7.3.5 VALIDATION

In the model test, the pressure outcome was validated by comparison with the full-scale CFD simulation as the conventional method to assess outdoor wind conditions. CFD was selected for three reasons. First, its capacities respond to the identified issues in the existing wind downscaling as explained in Chapter 1. Second, CFD is the method that was used to assess the urban context samples in the database development for both pressure and speed, especially with the same geometries and material. Third, CFD has become widely accepted in urban scale studies for its improved credibility and practicality, compared to other methods such as wind tunnel experiments or field surveys.

However, wind tunnel experiments are considered a more accurate method, because aerodynamic forces on the physical model are measured directly. The urban context samples can be evaluated more realistically, which can be used to validate the settings of CFD simulation, especially with its computational domain, turbulence models and meshing. In this way, the proposed model can be calibrated for higher accuracy toward the real world performances.

7.4 CONCLUDING REMARK

In this conclusion chapter, several further studies have been proposed to reduce uncertainties in the proposed wind downscaling model. However, as has been argued throughout the case studies, the proposed model has demonstrated accurate yet high-speed prediction, appropriate for the design area of interest in early stages. Especially, the effective use for the neighborhood scale would reduce uncertainties in climate-conscious design researches, by comprehensively assessing urban contexts to predict local wind speed and surface wind pressure.

In order to go beyond the proposed model and its output wind data, however, other climatic variables, such as temperature and humidity, can be considered. If these climate variables were downscaled to represent local urban contexts, urban heat island effect would be better understood, together with wind data. One possible solution is to reuse the presented methodological framework for other climatic variables. Air temperature, for instance, can be predicted for sample urban conditions by using extended thermal capacities of CFD. Even though the required integration of thermal and wind models in CFD adds more computation burdens, users' run-time would not be noticeably affected as demonstrated for wind. A temperature database, consequently, may be constructed and used for predictions with the employed techniques in the dissertation, meanwhile reusing geometries and materials. Therefore, the use of the proposed model can be expanded to conduct more robust design studies toward more efficient yet healthier environments.

BIBLIOGRAPHY

- AASHTO. 2001. "Policy on Geometric Design of Highways and Streets." American Association of State Highway and Transportation Officials, Washington, DC no. 1:990.
- Abbott, M. B. , and D. R. Basco. 1989. *Computational Fluid Dynamics – An Introduction for Engineers*: Longman Scientific & Technical, Harlow.
- Allegri, J., V. Dorer, and J. Carmeliet. 2012. "Influence of the urban microclimate in street canyons on the energy demand for space cooling and heating of buildings." *Energy and Buildings*.
- ANSYS. 2009. "Fluent 14.0 Documentation." *Ansys Inc*.
- Arnfield, A.J. 2003. "Two decades of urban climate research: a review of turbulence, exchanges of energy and water, and the urban heat island." *International Journal of Climatology* no. 23 (1):1-26.
- ASCE. 2003. Minimum Design Loads for Buildings and Other Structures.
- ASHRAE. 1993. "Fundamentals. 1993." American Society of Heating, Refrigerating, and Air Conditioning Engineers, Atlanta.
- ASHRAE. 2001. "Airflow around Buildings." In *ASHRAE fundamentals handbook*
- ASHRAE. 2009. Fundamentals Handbook. In *IP Edition*.
- Baker, Nick, and Koen Steemers. 2003. Energy and environment in architecture: a technical design guide: Taylor & Francis.
- Baklanov, A.A., and RB Nuterman. 2009. "Multi-scale atmospheric environment modelling for urban areas." *Adv. Sci. Res* no. 3:53-57.
- Becerra, Lucia. 2010. "Americans With Disabilities Act 2010 ADA Standards."
- Bern, Marshall Wayne, and Paul E Plassmann. 1997. *Mesh generation*: Pennsylvania State University, Department of Computer Science and Engineering, College of Engineering.
- Blocken, B., T. Stathopoulos, and J. Carmeliet. 2011. "Application of CFD in building performance simulation for the outdoor environment: an overview." *Journal of Building Performance Simulation* no. 4 (2):157-184.
- Blocken, Bert, Ted Stathopoulos, Jan Carmeliet, and Jan LM Hensen. 2011. "Application of computational fluid dynamics in building performance simulation for the outdoor

- environment: an overview." *Journal of Building Performance Simulation* no. 4 (2):157-184.
- Bouhaddou, H, MM Hassani, A Zeroual, and AJ Wilkinson. 1997. "Stochastic simulation of weather data using higher order statistics." *Renewable energy* no. 12 (1):21-37.
- Bulirsch, Roland, and Josef Stoer. 2002. *Introduction to numerical analysis*: Springer Heidelberg.
- Casella, George, and Roger L Berger. 2002. *Statistical inference*. Vol. 2: Duxbury Pacific Grove, CA.
- Cermak, Jack E. 1971. "Laboratory simulation of the atmospheric boundary layer." *AIAA Journal* no. 9 (9):1746-1754.
- Clarke, J A. 2001. *Energy Simulation in Building Design*. Woburn, MA: Butterworth-Heinemann.
- Cochran, William G. 2007. *Sampling techniques*: John Wiley & Sons.
- Crawley, D.B. 1998. "Which weather data should you use for energy simulations of commercial buildings?" *TRANSACTIONS-AMERICAN SOCIETY OF HEATING REFRIGERATING AND AIR CONDITIONING ENGINEERS* no. 104:498-515.
- Daley, Richard M. . 2007. *Street and Site Plan Design Standards*. edited by Chicago Department of Transportation. Chicago: City of Chicago.
- Davenport, AG, and HY Hui. 1982. "External and Internal Wind Pressures on Claddings of Buildings." *Boundary Layer Wind Tunnel Laboratory, University of Western Ontario, London, Canada*.
- de Berg, Mark, Otfried Cheong, Marc van Kreveld, and Mark Overmars. 2008. "Delaunay triangulations." *Computational Geometry: Algorithms and Applications*:191-218.
- Degelman, Larry. 2003. "Simulation and uncertainty." *Advanced building simulation*:60.
- DOE, US. 2005. *EnergyPlus Engineering Reference: The Reference to EnergyPlus Calculations*. US Department of Energy.
- DOE, US. 2010. *EnergyPlus Input Output Reference*. US Department of Energy, April.
- Duthinh, Dat, and Emil Simiu. 2011. *The Use of Wind Tunnel Measurements in Building Design*: INTECH Open Access Publisher.
- Dyrbye, Claës, and Svend Ole Hansen. 1997. *Wind loads on structures*.
- Feigenwinter, C., R. Vogt, and E. Parlow. 1999. "Vertical structure of selected turbulence characteristics above an urban canopy." *Theoretical and Applied Climatology* no. 62 (1):51-63.
- Ferreira, AD, AMG Lopes, DX Viegas, and ACM Sousa. 1995. "Experimental and numerical simulation of flow around two-dimensional hills." *Journal of wind engineering and industrial aerodynamics* no. 54:173-181.

- Feustel, HE, and A Rayner-Hoosen. 1990. "COMIS Fundamentals, LBL-28560." Applied Science Division, Lawrence Berkeley National Laboratory, Berkeley, CA. This work has been supported by the US Department of Energy via a subcontract with Carnegie Mellon University. The authors want to express their appreciation for the generous assistance of Nina Baird and Fred Betz.
- Filipova, BLANKA, and RADOVAN Hajovsky. 2011. Using MATLAB for modeling of thermal processes in a mining dump. Paper read at Proceedings of the 9th IASME/WSEAS International Conference on Heat Transfer, Thermal Engineering and Environment.
- Franke, J. 2006. Recommendations of the COST action C14 on the use of CFD in predicting pedestrian wind environment.
- Freedman, David. 2009. *Statistical models: theory and practice*: Cambridge University Press.
- Gu, Lixing. 2007. Airflow network modeling in EnergyPlus. Paper read at BUILDING SIMULATION.
- Haeger-Eugensson, Marie, and Björn Holmer. 1999. "Advection caused by the urban heat island circulation as a regulating factor on the nocturnal urban heat island." *International Journal of Climatology* no. 19 (9):975-988.
- Hamming, Richard. 2012. *Numerical methods for scientists and engineers*: Courier Dover Publications.
- Hensen, Jan LM, and Roberto Lamberts. 2011. *Building performance simulation for design and operation*: Taylor & Francis US.
- Hensen, Jan LM, and Roberto Lamberts. 2012. *Building performance simulation for design and operation*: Routledge.
- Hewitson, BC, and RG Crane. 1996. "Climate downscaling: techniques and application." *Climate Research* no. 7 (2):85-95.
- Hoare, Charles Antony Richard. 1969. "An axiomatic basis for computer programming." *Communications of the ACM* no. 12 (10):576-580.
- Incropera, Frank P. 2011. *Fundamentals of heat and mass transfer*: John Wiley & Sons.
- Iyer, Manjula A, and Layne T Watson. 2006. "An interpolation method for high dimensional scattered data." *SIMULATION SERIES* no. 38 (2):217.
- Jebson, S. 2007. "Fact sheet number 14: Microclimates."
- Johnson, GT, and LJ Hunter. 1998. "Urban wind flows: wind tunnel and numerical simulations—a preliminary comparison." *Environmental modelling & software* no. 13 (3):279-286.

- Johnson, GT, TR Oke, TJ Lyons, DG Steyn, ID Watson, and JA Voogt. 1991. "Simulation of surface urban heat islands under "ideal conditions at night Part 1: theory and tests against field data." *Boundary-Layer Meteorology* no. 56 (3):275-294.
- Kahaner, David, Cleve Moler, and Stephen Nash. 1989. "Numerical methods and software." *Englewood Cliffs: Prentice Hall, 1989* no. 1.
- Kaye, David H, and David A Freedman. 2000. "Reference guide on statistics." *Reference manual on scientific evidence* no. 83:102-04.
- Kim, J., Y. K. Yi, and A.M. Malkawi. 2011. Building Form Optimization in Early Design Stage to Reduce Adverse Wind Condition, Using Computational Fluid Dynamics. Paper read at 12th Conference of International Building Performance Simulation Association, at Sydney, Australia.
- Kolarevic, Branco. 2003. Computing the performative in architecture. Paper read at Proceedings of the 21th eCAADe Conference: Digital Design. Graz, Austria.
- Larsen, Larissa. 2011. "Green Building and Climate Resilience." *Ann Arbor* no. 1001:48109.
- Malkin, Stuart. 2009. Weather Data for Building Energy Analysis.
- Marion, William, and Ken Urban. 1995. User's Manual for TMY2s: Typical Meteorological Years: Derived from the 1961-1990 National Solar Radiation Data Base: National Renewable Energy Laboratory.
- Martilli, Alberto. 2007. "Current research and future challenges in urban mesoscale modelling." *International Journal of Climatology* no. 27 (14):1909-1918.
- Masson, V. 2006. "Urban surface modeling and the meso-scale impact of cities." *Theoretical and Applied Climatology* no. 84 (1):35-45.
- Masson, Valery. 2000. "A physically-based scheme for the urban energy budget in atmospheric models." *Boundary-Layer Meteorology* no. 94 (3):357-397.
- McNeel, Robert. 2010. "RhinoCERES-NURBS Modelling for Windows (version 4)." *Available from: Seattle, WA, USA: McNeel North America www.rhino3d.com.*
- Mirzaei, Parham A, and Fariborz Haghghat. 2010. "Approaches to study urban heat island—abilities and limitations." *Building and Environment* no. 45 (10):2192-2201.
- Monedero, Javier. 2000. "Parametric design: a review and some experiences." *Automation in Construction* no. 9 (4):369-377.
- Monin, AS, and AMf Obukhov. 1954. "Basic laws of turbulent mixing in the surface layer of the atmosphere." *Contrib. Geophys. Inst. Acad. Sci. USSR* no. 151:163-187.
- Murakami, Shuzo, Ryoza Ooka, Akashi Mochida, Shinji Yoshida, and Kim Sangjin. 1999. "CFD analysis of wind climate from human scale to urban scale." *Journal of wind engineering and industrial aerodynamics* no. 81 (1-3):57-81. doi: 10.1016/s0167-6105(99)00009-4.

- Murphy, James. 1999. "An evaluation of statistical and dynamical techniques for downscaling local climate." *Journal of Climate* no. 12 (8):2256-2284.
- NEN. 2006. "Wind comfort and wind danger in the built environment NEN 8100 Dutch Standard."
- Niemann, Hans-Jürgen. 1993. "The boundary layer wind tunnel: an experimental tool in building aerodynamics and environmental engineering." *Journal of Wind Engineering and Industrial Aerodynamics* no. 48 (2):145-161.
- Oke, T.R. 1987. *Boundary layer climates*: Routledge.
- Oke, TR. 1976. "The distinction between canopy and boundary-layer urban heat islands." *Atmosphere* no. 14 (4):268-277.
- Oke, TR, and Conrad East. 1971. "The urban boundary layer in Montreal." *Boundary-Layer Meteorology* no. 1 (4):411-437.
- Oke, TR, and GB Maxwell. 1975. "Urban heat island dynamics in Montreal and Vancouver." *Atmospheric Environment (1967)* no. 9 (2):191-200.
- Oleson, K.W., GB Bonan, J. Feddema, and M. Vertenstein. 2008. "An urban parameterization for a global climate model. Part II: Sensitivity to input parameters and the simulated urban heat island in offline Simulations." *Journal of Applied Meteorology and Climatology* no. 47 (4):1061-1076.
- Park, H.S. 1986. "Features of the heat island in Seoul and its surrounding cities." *Atmospheric Environment (1967)* no. 20 (10):1859-1866.
- Powell, K. 2006. *30 St Mary Axe: A Tower for London*: Merrell Publishers.
- Ratti, Carlo. 2002. *Urban analysis for environmental prediction*, University of Cambridge.
- Ratti, Carlo, Nick Baker, and Koen Steemers. 2005. "Energy consumption and urban texture." *Energy and buildings* no. 37 (7):762-776.
- Rizwan, Ahmed Memon, Leung YC Dennis, and LIU Chunho. 2008. "A review on the generation, determination and mitigation of Urban Heat Island." *Journal of Environmental Sciences* no. 20 (1):120-128.
- Roller, Dieter. 1991. "An approach to computer-aided parametric design." *Computer-Aided Design* no. 23 (5):385-391.
- Saneinejad, S., J. Allegrini, V. Dorer, and J. Carmeliet. 2012. "Analysis of convective heat transfer at building façades in street canyons and its influence on the predictions of space cooling demand in buildings." *Journal of wind engineering and industrial aerodynamics*.
- Sanguinetti, P., and C. Kraus. 2011. "Thinking in Parametric Phenomenology." *DO NOT PRINT*:19.

- Santamouris, M. 2001. "Heat-island effect." *Energy and Climate Change in the Urban Built Environment*. Earthscan, London:48-68.
- Semenov, M.A., and R.J. Brooks. 1999. "Spatial interpolation of the LARS-WG stochastic weather generator in Great Britain." *Climate Research* no. 11:137-148.
- Shuzo, Murakami. 1997. "Current status and future trends in computational wind engineering." *Journal of wind engineering and industrial aerodynamics* no. 67,Äi68 (0):3-34. doi: 10.1016/s0167-6105(97)00230-4.
- Sierputowski, P, J Ostrowski, and A Cenedese. 1995. "Experimental study of wind flow over the model of a valley." *Journal of wind engineering and industrial aerodynamics* no. 57 (2):127-136.
- Simionescu, Petru-Aurelian, and David Beale. 2004. "Visualization of hypersurfaces and multivariable (objective) functions by partial global optimization." *The Visual Computer* no. 20 (10):665-681.
- Simiu, Emil. 2009. "Toward a standard on the wind tunnel method." *NIST Technical Note* no. 1655.
- Stathopoulos, Theodore. 1984. "Wind loads on low-rise buildings: a review of the state of the art." *Engineering Structures*
- Stathopoulos, Theodore. 2002. "The numerical wind tunnel for industrial aerodynamics: Real or virtual in the new millennium?" *WIND STRUCT INT J* no. 5 (2):193-208.
- Steiner, Frederick, and Kent Butler. 2006. *Planning and urban design standards*: John Wiley & Sons.
- Strachan, PA, G Kokogiannakis, and IA Macdonald. 2008. "History and development of validation with the ESP-r simulation program." *Building and Environment* no. 43 (4):601-609.
- Sun, Y., Y. Heo, H. Xie, M. Tan, J. Wu, and G. Augenbroe. 2011. *Uncertainty Quantification of Microclimate Variables in Building Energy Simulation*.
- Takahashi, Kazuya, Harunori Yoshida, Yuzo Tanaka, Noriko Aotake, and Fulin Wang. 2004. "Measurement of thermal environment in Kyoto city and its prediction by CFD simulation." *Energy and Buildings* no. 36 (8):771-779.
- Tominaga, Yoshihide, Akashi Mochida, Ryuichiro Yoshie, Hiroto Kataoka, Tsuyoshi Nozu, Masaru Yoshikawa, and Taichi Shirasawa. 2008. "AIJ guidelines for practical applications of CFD to pedestrian wind environment around buildings." *Journal of wind engineering and industrial aerodynamics* no. 96 (10):1749-1761.

- Troude, F, E Dupont, B Carissimo, and Al Flossmann. 2002. "Relative influence of urban and orographic effects for low wind conditions in the Paris area." *Boundary-Layer Meteorology* no. 103 (3):493-505.
- Versteeg, Henk Kaarle, and Weeratunge Malalasekera. 2007. *An introduction to computational fluid dynamics: the finite volume method*: Pearson Education.
- Walton, George N. 1989. *AIRNET: A Computer Program for Building Airflow Network Modeling*: National Institute of Standards and Technology Gaithersburg, USA.
- Wanner H., Filliger P 1989. "Orographical influence on urban climate." *Weather and Climate* 9: 22–28.
- WHO. 2008. "Climate change and health."
- Wilcox, David C. 1998. *Turbulence modeling for CFD*. Vol. 2: DCW industries La Canada, CA.
- Wilcox, Stephen, and William Marion. 2008. *Users manual for TMY3 data sets*: National Renewable Energy Laboratory Golden, CO.
- Willemsen, Eddy, and Jacob A Wisse. 2007. "Design for wind comfort in The Netherlands: Procedures, criteria and open research issues." *Journal of Wind Engineering and Industrial Aerodynamics* no. 95 (9):1541-1550.
- Wilson, DJ. 1989. "Airflow around buildings." *ASHRAE handbook of fundamentals* no. 14:1-14.
- Woodbury, Robert. 2010. "Elements of parametric design."
- Yao, R., Q. Luo, and B. Li. 2011. "A simplified mathematical model for urban microclimate simulation." *Building and Environment* no. 46 (1):253-265.
- Yi, YK, and AM Malkawi. 2009. "Optimizing building form for energy performance based on hierarchical geometry relation." *Automation in Construction* no. 18 (6):825-833.
- Zezula, Pavel, Giuseppe Amato, Vlastislav Dohnal, and Michal Batko. 2006. *Similarity search: the metric space approach*. Vol. 32: Springer.
- Zhai, Z. 2006. "Application of computational fluid dynamics in building design: aspects and trends." *Indoor and built environment* no. 15 (4):305-313.
- Zhao, Chongbin, Bruce E Hobbs, and Alison Ord. 2008. *Convective and advective heat transfer in geological systems*: Springer.

INDEX

A

AASHTO44
acceptable range of errors 16, 25
airflow 7, 10, 11
airflow rate10
American Disability Act.....44
ASHRAESee the American Society of
Heating, Refrigerating, and Air-
Conditioning Engineers
atmospheric boundary layer parameters24

B

Bernoulli's39
building-averaged66

C

canyon9
CFD.12, 18, 31, 51, 59, 60, 61, 66, 76, 85,
88
computational lightness.....37
computer-aided design modeling29

D

database 4, 32, 38, 47
Delaunay triangulation..... 37, 50

design syntheses..... 12
downscaling.....5, 6, 7, 8

E

early design stages9, 66
EnergyPlus 11, 16

F

field surveys.....95
flexible parameters30, 43

G

geometric sensitivity88
geometric variables 17
geometrical sensitivity 13, 91
griddatan.....50

H

heat balance 1
heat island effect9, 96
heterogeneities92
hierarchies of pressure intensities26
high-dimensional problems37
homogenous terrain8

I

interpolation 15, 16, 36, 38, 45, 52

K

K-epsilon Renormalized Group32

L

leeward 5, 9, 65

life spans of buildings4

link..... 10, 11

localization5

M

MATLAB50

meshing 32, 70, 95

Monin-Obukhov Similarity Theory10

N

neighborhood height..... 31, 45

neighborhood length.....60

neighborhood scale 8, 43

neighborhood volume.... 17, 31, 42, 77, 90

nodal model10

nodal network10

node..... 10, 11

O

outdoor nodal model.....11

P

parameterization..... 18

pertinence..... 14, 88

prism layers32

proximity search38, 56, 57

R

range of errors 60

regional scale4, 94

Reynolds Averaged Navier-Stokes 32

S

sampling30, 46

skewedness.....37

skyscrapers66

slopesi, 44, 69, 77, 81

smoothness32

surface orientations.....49

T

the American Society of Heating,
Refrigerating, and Air-Conditioning
Engineers67

the second order upwind32

TMY See Typical Meteorological Year

topographic effect.....7, 18, 90

turbulences 18

Typical Meteorological Year4

U

urban boundary layer.....	9, 12, 90
urban boundary layer thicknesses.....	24
urban climatology	3
urban constructions	5
urban context.....	i, 1, 16, 28, 41, 89
urban designs	2
urban topographies.....	25

V

virtual wind tunnel test.....	18, 25, 67
-------------------------------	------------

W

wind downscaling	5, 16, 87
wind pressure	14, 17, 36, 47, 76, 87
wind reduction ratios	67, 74
wind tunnel experiments	12, 25, 31